-131

NATIONAL ADVISORY COMMITTEE FOR AERONAUTICS

WARTIME REPORT

ORIGINALLY ISSUED

November 1945 as
Advance Restricted Report E5J31

HEAT-TRANSFER PROCESSES IN LIQUID-COOLED ENGINE CYLINDERS

I - CORRELATION OF SINGLE-CYLINDER ENGINE TEMPERATURES UNDER FORCED-CONVECTION COOLING CONDITIONS

By Benjamin Pinkel, Eugene J. Manganiello
and Everett Bernardo

Aircraft Engine Research Laboratory
Cleveland, Ohio

WASHINGTON

NACA ARR No. E5J31

NATIONAL ADVISORY COMMITTEE FOR AERONAUTICS

ADVANCE RESTRICTED REPORT

HEAT-TRANSFER PROCESSES IN LIQUID-COOLED ENGINE CYLINDERS

I - CORRELATION OF SINGLE-CYLINDER ENGINE TEMPERATURES UNDER FORCED-CONVECTION COOLING CONDITIONS

By Benjamin Pinkel, Eugene J. Manganiello
and Everett Bernardo

SUMMARY

An analysis based on forced-convection heat-transfer theory, similar to the analysis presented for air-cooled engines in NACA Report No. 612, is made of the cooling processes in liquid-cooled engine cylinders. Semiempirical equations that relate the average head and barrel temperatures with the primary engine and coolant parameters are derived.

A correlation method based on these equations is applied to data obtained from previously reported tests, which were conducted over large ranges of engine and coolant conditions with two liquid-cooled cylinders using water and various aqueous ethylene glycol solutions as coolants. An equation for the cylinder-head temperature as a function of the engine operating conditions and the flow rate, temperature, and physical properties of the coolants is obtained, which represents the test data with good accuracy. A similar equation is obtained for the barrel-temperature data. The physical properties of the coolant appearing in these equations in order of their importance in determining the heat-transfer quality of the coolant are the thermal conductivity, the specific heat, and the viscosity. The cooling performance of the various coolants investigated is adequately correlated by these physical properties in the correlation equation. The application of the correlation equation is, however, limited to conditions for which boiling of the coolant on the engine walls is not an important part of the cooling process.

INTRODUCTION

Recent and projected improvement in the power output of liquid-cooled aircraft engines has stimulated interest in the cooling

characteristics of these engines and has emphasized the desirability of obtaining a method of correlating cylinder temperatures with engine and coolant conditions.

In 1937 the heat-transfer processes in air-cooled engine cylinders were analyzed and a method based on forced-convection heat-transfer theory was developed for correlating cylinder temperatures with engine and cooling-air conditions (reference 1). This method was extended in 1939 to include multicylinder-engine data (reference 2).

In 1943 an experimental investigation of the cooling characteristics of a multicylinder liquid-cooled engine was instituted at the Cleveland laboratory of the NACA. As a supplement to this investigation, tests were conducted with two liquid-cooled cylinders to isolate the effects of the different engine and coolant variables on cylinder temperatures and to obtain the data required for a study of the fundamental heat-transfer processes involved in the cooling of liquid-cooled engines. The cylinder temperatures, which were obtained over ranges of engine speeds, manifold pressures, carburetor-air temperatures, fuel-air ratios, spark advances, coolant-flow rates, coolant temperatures, and coolant pressures with water and with various ethylene glycol-water mixtures, are presented in reference 3.

In the present report the theory of heat transfer by forced convection is applied to the cooling processes in a liquid-cooled engine cylinder. The method of analysis is essentially the same as that used in reference 1 for air-cooled engines with the additional complications: (1) that the variation of Prandtl number of the coolant with coolant temperature and composition, which was negligible for the air-cooled engine, becomes an important consideration for the liquid-cooled engine, and (2) that, because the ratio of the temperature drop through the engine wall to the temperature difference between the wall and the coolant is large for the liquid-cooled engine, an additional term must be introduced into the correlation equation.

The analysis results in semiempirical expressions for the average head and barrel temperatures as functions of the engine conditions and the temperature, the flow rate, and the physical properties of the coolant. The physical properties of the coolant that appear in this equation are the thermal conductivity, the specific heat, and the viscosity; and in the region of operation, where forced convection is the controlling cooling phenomenon, correlation of the cooling performance of various coolants on the basis of these coolant physical properties can be expected. In the test range where appreciable boiling of the coolant occurs on the engine walls the correlation equation developed herein can be expected to be inaccurate.

The cooling correlation method is applied to the data presented in reference 3.

SYMBOLS

$\bar{A}$	mean area of cylinder wall perpendicular to direction of heat flow, (sq ft)
A_l	cylinder-wall area in contact with coolant, (sq ft)
B_1, $B_2 \ldots B_9$	constants
c	specific heat of coolant, (Btu)/(lb)($^\circ$F)
D	hydraulic diameter, (ft)
h	heat-transfer coefficient, liquid side, (Btu)/(sec)(sq ft)($^\circ$F)
H_b	heat rejected to barrel coolant, (Btu)/(min)
H_h	heat rejected to head coolant, (Btu)/(min)
k	thermal conductivity of coolant, (Btu)/(sec)(sq ft)($^\circ$F/ft)
k_w	thermal conductivity of cylinder wall, (Btu)/(sec)(sq ft)($^\circ$F/ft)
m, n, s	exponents
T_{b_o}	average cylinder-barrel (liquid-side) temperature, ($^\circ$F)
T_g	effective cylinder-gas temperature, ($^\circ$F)
T_h	average cylinder-head (gas-side) temperature, ($^\circ$F)
T_{h_o}	average cylinder-head (liquid-side) temperature, ($^\circ$F)
T_l	average coolant temperature, ($^\circ$F)
V	coolant linear velocity, (ft)/(sec)
W_l	coolant-flow rate, (lb)/(min)
W_c	charge (air plus fuel) flow rate, (lb)/(min)

x	mean thickness of cylinder head parallel to direction of heat flow, (ft)
Z	$(B_1 x/B_2 k_w \bar{A})$
ρ	density of coolant, (lb)/(cu ft)
μ	absolute viscosity of coolant, (lb)/(ft)(sec)
$c\mu/k$	Prandtl number

ANALYSIS

The analysis of the heat-transfer processes in a liquid-cooled engine cylinder is separated into three processes: the heat transfer (1) from the cylinder gases to the gas-side cylinder walls, (2) through the cylinder walls, and (3) from the liquid-side cylinder walls to the coolant. A diagrammatic sketch of a liquid-cooled engine cylinder illustrating the various sections is shown in figure 1.

Heat Transfer in the Cylinder Head

Cylinder gases to gas-side cylinder wall. - The transfer of heat from the cylinder gases to the walls may be expected to be the same for liquid-cooled engines as for air-cooled engines; hence, an expression based on forced-convection heat-transfer theory similar to that derived in reference 1 may be written

$$H_h = B_1 W_c^n (T_g - T_h) \tag{1}$$

Conduction through cylinder walls. - The heat transferred through the cylinder walls follows the laws of conduction and may be expressed

$$H_h = B_2 \frac{k_w \bar{A}}{x} \left(T_h - T_{h_o}\right) \tag{2}$$

Liquid-side cylinder walls to coolant. - For a large part of the interesting operating range cooling of the engine walls occurs by forced convection. In this range of operation the following familiar Nusselt relation may be written

$$\frac{hD}{k} = B_3 \left(\frac{\rho VD}{\mu}\right)^m \left(\frac{c\mu}{k}\right)^s \tag{3}$$

When appreciable boiling of the coolant on the engine walls occurs, deviation of the heat-transfer coefficient from the value given by

equation (3) may be expected. The analysis will be continued on the basis of equation (3). The final correlation equation will then apply to operating conditions where forced convection controls the heat-transfer process. Deviations from the correlation equation will indicate regions in which other modes of heat transfer become important. For a given engine D in equation (3) is constant; $\rho V D$ is proportional to W_l; and, since h is defined as $\frac{H_h}{B_2 A_l (T_{h_o} - T_l)}$, the heat flow per unit time is

$$H_h = B_4 \, k \left(\frac{W_l}{\mu}\right)^m \left(\frac{c\mu}{k}\right)^s \left(T_{h_o} - T_l\right) \tag{4}$$

Correlation equation. - The correlation equation is obtained by eliminating H_h and T_{h_o} from equations (1), (2), and (4):

$$\left[\frac{T_h - T_l}{W_c^n (T_g - T_h)} - Z\right] \left(\frac{c\mu}{k}\right)^s k = B_5 \left(\frac{W_l}{\mu}\right)^{-m} \tag{5a}$$

where $Z = B_1 x/B_2 k_w \bar{A}$ and accounts, in effect, for the temperature drop through the cylinder-head wall. Inasmuch as the thermal conductivity of the cylinder-head metal k_w is effectively constant for the temperature range encountered in normal engine operation, Z may be taken as a constant for a given engine.

An alternative form of the final equation (5a) involving both gas-side and liquid-side head temperatures can be obtained by eliminating H_h from equations (1) and (4):

$$\frac{T_{h_o} - T_l}{W_c^n (T_g - T_h)} \left(\frac{c\mu}{k}\right)^s k = B_5 \left(\frac{W_l}{\mu}\right)^{-m} \tag{5b}$$

For correlation of the data for any one coolant, equation (5a) is simplified by expressing c, μ, and k as a function of T_l:

$$\left[\frac{T_h - T_l}{W_c^n (T_g - T_h)} - Z\right] W_l^m = B_5 \frac{\mu^{(m-s)}}{c^s k^{(1-s)}} = B_5 \, f(T_l) \tag{5c}$$

Heat Transfer in the Cylinder Barrel

The heat-transfer processes in the cylinder barrel are expected to be the same as those in the head except that (a) the temperature drop through the barrel wall is so relatively small that the Z factor may be omitted, and (b) the simple application of the theory of forced convection to the heat transfer from the cylinder gases to the barrel wall, as shown in reference 1, is only a rough approximation because the process is complicated by the generation and the transfer of heat by the piston. In the interest of simplicity, consideration of the complications introduced by the piston is neglected and the relation for the over-all heat transfer in the cylinder barrel is written in a form similar to that for the cylinder head:

$$\frac{T_{b_o} - T_l}{W_c^{\,n}\left(T_g - T_{b_o}\right)}\left(\frac{c\mu}{k}\right)^s k = B_6\left(\frac{W_l}{\mu}\right)^{-m} \qquad (6a)$$

Equation (6a) is simplified as follows for correlating the data for any one coolant:

$$\frac{T_{b_o} - T_l}{W_c^{\,n}\left(T_g - T_{b_o}\right)} W_l^{\,m} = B_6\, f\,(T_l) \qquad (6b)$$

SIGNIFICANCE OF EQUATIONS AND CONSTANTS

Equations (5a), (5b), and (6a) are the final equations for correlating the cylinder-temperature data with the engine and coolant variables. When the left-hand member of any of these equations is plotted on logarithmic coordinates against W_l/μ, a single curve should be obtained for a given engine regardless of the engine conditions or the temperature, flow rate, and composition of the coolant used, provided that modes of heat transfer other than forced convection are of negligible magnitude. Systematic deviation of the test points from the common correlation curve will indicate the presence and the importance of other modes of heat transfer or of variables not included in the final equations.

The effective gas temperature T_g, as indicated in references 1 and 2, is a function of fuel-air ratio, carburetor-air temperature,

spark advance, and exhaust back pressure. The values of T_g for the head and for the barrel, as well as the variation of T_g with fuel-air ratio, carburetor-air temperature, and spark advance, is obtained from engine tests as will subsequently be described. The variation of T_g with exhaust back pressure is not discussed inasmuch as data on variable exhaust back pressure were not available.

The factors Z, B_5, and B_6 and the exponents m, n, and s are also determined from engine tests. The details of evaluating these terms are presented in a later section. Although the symbols used in the head equations for the effective gas temperature, the average coolant temperature, the coolant-flow rate, and the exponents are the same as those used in the barrel equations, the numerical values of these factors are not necessarily the same for the head and the barrel.

The physical properties c, μ, and k of the coolants are, of course, functions of coolant composition and temperature. Curves of c, μ, and k as functions of temperature for water and for ethylene glycol-water mixtures are presented later in this report.

APPARATUS AND TESTS

The data presented in reference 3, which are used herein, were obtained from two modified Lycoming O-1230 liquid-cooled cylinders, cylinder A and cylinder B. A detailed description of the setup, the methods, and the results obtained is given in reference 3. The general arrangement of the engine and the auxiliary equipment is shown in figure 2. Diagrams of cylinder A and cylinder B, which are the same except for the cylinder-barrel instrumentation and the coolant-flow paths, are presented in figure 3. In cylinder A the barrel-coolant jacket was modified and eight thermocouples were spot-welded around the barrel. In addition, the coolant-transfer passages between the head and barrel jackets were plugged, thus separating the coolant flow to the head and barrel. In cylinder B thermocouples were not installed on the barrel and the coolant-flow paths were not altered; hence, the coolant flowed first through the barrel and then through the head. The following table is a compilation of the test conditions investigated:

Variable	Range of variable	Coolant, glycol-water (approximate percent by volume)[a]	Cylinder
Engine speed, rpm	1050 to 2760	[b]97-3	A and B
		0-100	B
Manifold pressure, in. Hg absolute	21.0 to 39.0	[b]97-3	A and B
		0-100	B
Carburetor-air temperature, °F	80 to 222	[b]97-3	A
Fuel-air ratio	0.048 to 0.121	[b]97-3	A
		0-100	B
Spark advance, deg B.T.C.	12 to 42	[b]97-3	A
Coolant-flow rate, lb/min	10.0 to 128.3	[b]97-3	A and B
		70-30	A and B
		30-70	A and B
		0-100	A and B
Average coolant temperature, °F	90.0 to 311.0	[b]97-3	A and B
		70-30	A and B
		30-70	A and B
		0-100	A and B
Coolant pressure, lb/sq in. absolute	17 to 75	0-100	A

[a]The ethylene glycol-water mixture used in several tests conducted with cylinder A was actually 38 percent-62 percent instead of 30 percent-70 percent.

[b]AN-E-2 ethylene glycol.

In each of the tests only one item was varied while all of the others were held approximately constant. (In one test both coolant temperature and flow rate were varied simultaneously.) The following conditions were held approximately constant throughout the investigation except for the cases in which the particular condition was the primary variable:

Coolant pressure, pounds per square inch absolute 19
Exhaust back pressure, inches of mercury absolute 30
Carburetor-air temperature, °F . . . . . 80 ±5
Fuel-air ratio . . . . . 0.077 ±0.001
Spark advance, degrees B.T.C. 28

Several tests conducted with cylinder A were repeated at higher coolant pressures and in the tests of cylinder B each run was repeated at a higher coolant pressure.

METHODS

Evaluation of Factors for Correlation Equations

In most cases the data used herein for evaluating the exponents and constants are from cylinder A inasmuch as all the variables were investigated with this cylinder and, in addition, barrel temperatures were obtained.

Average temperatures. - The average temperatures used are those given in reference 3. The average head (gas-side) temperature T_h was taken as the average of values obtained from nine thermocouples (13 to 21, fig. 3) located in the cylinder head, approximately 1/8 inch from the combustion-chamber surface. The average head (liquid-side) temperature T_{h_o} was obtained from the arithmetic mean of values determined by four thermocouples (24 to 27, fig. 3) located on the liquid-side surface of the combustion-chamber wall. The average barrel (liquid-side) temperature T_{b_o} was taken as the average of readings obtained from eight thermocouples (1 to 8, fig. 3(a)) spot-welded on the outside of the barrel in two rows of four thermocouples each. The average of the coolant temperatures measured in the inlet and outlet coolant passages of each portion of the cylinder was used as the average coolant temperature T_l.

Physical properties of the coolants. - The thermal conductivity k, the absolute viscosity μ, and the specific heat c of water and of the glycol-water solutions are shown as functions of temperature in figures 4 and 5, respectively, (data of reference 4). The tests reported in reference 5 indicate that satisfactory correlation of forced-convection heat-transfer data for water and for aqueous ethylene glycol solutions is obtained using these values of the physical properties. The physical properties used in the final equations are evaluated at the value of the average coolant temperature T_l.

Effective gas temperature T_g. - The values of T_g for the head and the barrel are obtained from tests at reference conditions of fuel-air ratio, carburetor-air temperature, and spark advance in which only W_l and T_l were varied. The values of the heat rejected to the head and barrel coolant are plotted against T_h and T_{b_o}, respectively, and the curves extrapolated to zero heat rejection at which points the average head and barrel temperatures are

equal to their respective effective gas temperatures. (See equation (1).) Small differences in the choice of the initial or reference value of T_g do not seriously change the accuracy of the correlation. It is of greater importance, once the initial value of T_g is chosen, that the variation of T_g from the initial value with variation in fuel-air ratio, carburetor-air temperature, and spark advance be accurate.

The variation of T_g with fuel-air ratio, carburetor-air temperature, and spark advance is obtained from the results of the tests in which each of these factors was independently varied while holding the engine charge flow and the coolant conditions constant. For such conditions equations (5a) and (6a) reduce, respectively, to

$$\frac{T_h - T_l}{T_g - T_h} = \text{constant}$$

and

$$\frac{T_{b_o} - T_l}{T_g - T_{b_o}} = \text{constant}$$

These constants are evaluated from the cylinder-temperature and coolant-temperature data at the reference operating conditions for which T_g has already been determined. The value of T_g at other than the reference conditions is then calculated from the values of the constant, the constant coolant temperature, and the cylinder temperature obtained at the operating conditions in question.

Exponent n of charge-flow rate W_c. - The values of the exponent n of charge-flow rate W_c are obtained from tests at constant coolant conditions in which engine speed or manifold pressure, hence W_c, was varied.

For these test conditions equations (5a) and (6a) reduce to

$$\frac{T_h - T_l}{T_g - T_h} = B_7 W_c^n$$

and

$$\frac{T_{b_o} - T_l}{T_g - T_{b_o}} = B_8 W_c^n$$

Logarithmic plots of $\frac{T_h - T_l}{T_g - T_h}$ and $\frac{T_{b_o} - T_l}{T_g - T_{b_o}}$ against W_c are made and the values of the exponent obtained directly from the slopes of the resulting lines.

The factor Z. - The factor Z is evaluated from tests in which W_l was varied for different values of constant coolant temperature and composition. These conditions of constant coolant temperature and composition predicate constant c, μ, and k, in which case equation (5a) may be written:

$$\frac{T_h - T_l}{W_c^n (T_g - T_h)} - Z = B_9 \left(\frac{1}{W_l}\right)^m$$

Plots of $\frac{T_h - T_l}{W_c^n (T_g - T_h)}$ against $1/W_l$ are made and the curves obtained are extrapolated to zero $1/W_l$ (infinite W_l) at which point the value of $\frac{T_h - T_l}{W_c^n (T_g - T_h)}$ is equal to Z.

Exponent s of Prandtl number $c\mu/k$. - The value of the Prandtl number exponent s is determined from two successive logarithmic plots. First, $\left[\frac{T_h - T_l}{W_c^n (T_g - T_h)} - Z\right] k$ is plotted against W_l/μ, using data obtained from variable W_l tests conducted with different coolants at several temperature levels. Values of $\left[\frac{T_h - T_l}{W_c^n (T_g - T_h)} - Z\right] k$ are then cross-plotted against $c\mu/k$ at a constant value of W_l/μ, which results in a line with a negative slope equal in absolute value to the exponent s of the Prandtl number. (See equation (5a).)

Final Correlation

Final correlation plots of the engine-cooling data for all the coolants tested are obtained by plotting the following parameters against W_l/μ on logarithmic coordinates

(a) Head (gas-side) temperatures $\left[\frac{T_h - T_l}{W_c^{\,n}(T_g - T_h)} - Z\right]\left(\frac{c\mu}{k}\right)^s k$

(b) Head (gas-side and liquid-side) temperatures $\frac{T_{h_o} - T_l}{W_c^{\,n}(T_g - T_h)}\left(\frac{c\mu}{k}\right)^s k$

(c) Barrel (liquid-side) temperatures $\frac{T_{b_o} - T_l}{W_c^{\,n}\left(T_g - T_{b_o}\right)}\left(\frac{c\mu}{k}\right)^s k$

Data are included from the tests in which each of the various engine and coolant variables were investigated. The values of the exponent m of the coolant-flow-rate variable W_l/μ and of the constants B_5 and B_6, which complete the determination of the final correlation equations (5a), (5b), and (6a), are obtained from the slopes and the coordinates of the resulting lines.

In addition, separate correlation curves for each of the coolants tested are obtained by plotting $\left[\frac{T_h - T_l}{W_c^{\,n}(T_g - T_h)} - Z\right] W_l^{\,m}$ against T_l and $\frac{T_{b_o} - T_l}{W_c^{\,n}\left(T_g - T_{b_o}\right)} W_l^{\,m}$ against T_l. (See equations (5c) and (6b).)

RESULTS AND DISCUSSION

Factors for Correlation Equations

Effective gas temperature T_g. - Typical plots used for determining the reference values of T_g for the head and the barrel are shown in figure 6. The heat rejected to the head and the barrel coolant is plotted against T_h and T_{b_o}, respectively, from the results of tests conducted at a fuel-air ratio of 0.077, a carburetor-air temperature of 80° F, and a spark advance of 28° B.T.C. Values of T_g of 1170° F for the head and 610° F for the barrel are indicated by extrapolating the curves to zero heat rejection. Admittedly, a certain amount of latitude exists in the choice of these values in view of the extrapolated distance as compared with the range covered by the data; however, consideration of a large number of these curves for air-cooled engines (see reference 1) led to the values chosen.

The variation of T_g for the head and the barrel with fuel-air ratio is presented in figure 7, which includes data for the head from both cylinders A and B. Also shown in the figure are typical head T_g curves for air-cooled engines obtained from single-cylinder tests of a Wright R-1820-G engine (reference 2) and a Pratt & Whitney R-2800-21 engine (reference 6). Good agreement exists between the curves for the liquid-cooled and the air-cooled engines, especially in the rich-mixture region. The curves intersect values of T_g of 1150° F for the head and 600° F for the barrel at a fuel-air ratio of 0.08.

The effect of carburetor-air temperature on T_g is shown in figure 8. The data were obtained from tests conducted at fuel-air ratios of approximately 0.077 and 0.080. The data obtained at a fuel-air ratio of 0.080 are corrected to the reference value of 0.077. An increase in T_g of approximately 0.5° F and 0.15° F per °F increase in carburetor-air temperature is obtained for the head and the barrel, respectively.

Figure 9 shows the variation of T_g with spark advance at a fuel-air ratio of 0.077. The value of T_g for the head decreases about 300° F as the spark is retarded through a crank angle of 30°; the rate of change decreases slightly at the retarded position. The effect of spark setting on T_g for the barrel is not so pronounced as for the head and a small reversal is obtained at the late setting.

Exponent n of charge flow rate W_c. - Logarithmic plots of $\frac{T_h - T_l}{T_g - T_h}$ and $\frac{T_{b_o} - T_l}{T_g - T_{b_o}}$ against W_c are shown in figure 10, where the values of T_g are the previously determined reference values of 1170° F and 610° F for the head and the barrel, respectively. The slope of the average line through the data, which is equal to the exponent n, is 0.65. This value is in agreement with values obtained for several air-cooled cylinders. Although slightly varying slopes would be obtained from plots of individual test runs, the average line results in a good correlation of the data.

The factor Z. - A plot of $\frac{T_h - T_l}{W_c^{0.65}(T_g - T_h)}$ against $1/W_l$ is presented in figure 11 from the results of several tests conducted at different engine conditions using various coolants. Extrapolation of the different curves to zero $1/W_l$ results in a single value for Z equal to 0.017. The extrapolation, particularly of

the upper curves in the figure, may be considered somewhat arbitrary. Justification for the choice of this value for Z exists, however, in the good correlation of the data subsequently obtained.

Exponent s of Prandtl number $c\mu/k$. - The two logarithmic plots used for determining the exponent of the Prandtl number are presented in figure 12. Figure 12(a) shows $\left[\frac{T_h - T_l}{W_c^{0.65}(T_g - T_h)} - 0.017\right]k$ as a function of W_l/μ for several coolants at different constant average coolant temperatures. A family of approximately parallel lines (slopes from -0.55 to -0.60) is obtained. Figure 12(b) shows the variation of $\left[\frac{T_h - T_l}{W_c^{0.65}(T_g - T_h)} - 0.017\right]k$ with $c\mu/k$ as determined by cross-plotting from figure 12(a) at a value of W_l/μ equal to 80,000. A value for the exponent of $c\mu/k$ of 0.40 for the head is directly obtained from the absolute value of the slope of the resulting line. This value of the exponent is equal to that generally recommended for forced-convection heat transfer (reference 7); therefore, a value of 0.40 will also be used as the exponent for the barrel without further evaluation.

Final Correlation

Generalized correlation for all coolants. - The final generalized correlation plots, which include data for wide ranges of engine operating conditions, coolant temperatures, flow rates, and compositions, are presented in figures 13 to 16. In figures 13 and 14 the correlation parameters involving the gas-side head temperature for cylinders A and B, respectively, are plotted according to equation (5a). The slope of the average line through the data, which is equal to the exponent m of the coolant-flow-rate variable W_l/μ, is -0.6 for cylinder A and -0.5 for cylinder B. The difference in slope for cylinders A and B may be attributed to the difference in the coolant-flow conditions for the two cylinders. Except for a few cases the deviations of the data points from the line represent differences in average head temperature of less than $\pm 10^{\circ}$ F.

The correlation plot for the barrel of cylinder A (see equation (6a)) is shown in figure 15 and the slope of the resulting line is -0.55. Slightly more scatter is obtained for the barrel than for the head; the correlation, however, is considered good.

The equations for the lines obtained in the preceding plots are:

Head, cylinder A, figure 13

$$\left[\frac{T_h - T_l}{W_c^{0.65}\,(T_g - T_h)} - 0.017\right]\left(\frac{c\mu}{k}\right)^{0.4} \quad k = 0.00418\left(\frac{W_l}{\mu}\right)^{-0.6} \tag{7}$$

Head, cylinder B, figure 14

$$\left[\frac{T_h - T_l}{W_c^{0.65}\,(T_g - T_h)} - 0.017\right]\left(\frac{c\mu}{k}\right)^{0.4} \quad k = 0.00126\left(\frac{W_l}{\mu}\right)^{-0.5} \tag{8}$$

Barrel, cylinder A, figure 15

$$\frac{T_{b_o} - T_l}{W_c^{0.65}\,(T_g - T_{b_o})}\left(\frac{c\mu}{k}\right)^{0.4} \quad k = 0.00260\left(\frac{W_l}{\mu}\right)^{-0.55} \tag{9}$$

An alternative form of the correlation plot for the head involving both gas-side and liquid-side head temperatures (equation (5b)) is presented for cylinder A in figure 16. The slope of the average line through the data is -0.6, which agrees with that obtained in figure 13 for this cylinder. The equation for the line is

$$\frac{T_{h_o} - T_l}{W_c^{0.65}\,(T_g - T_h)}\left(\frac{c\mu}{k}\right)^{0.4} \quad k = 0.00345\left(\frac{W_l}{\mu}\right)^{-0.6} \tag{10}$$

The apparent difference in the value of the constant B_5 in equations (7) and (10) is attributed to the fact that the values of T_{h_o} used in this correlation are probably not representative of the true average liquid-side head temperature inasmuch as these temperatures were obtained from the readings of only four thermocouples. The values of T_{h_o} do, however, bear a linear relation to the average temperature. The data of reference 3 show that individual temperatures give a straight-line relation with average temperatures over the entire range of engine and coolant conditions.

Individual correlation for each coolant. - In figures 17 and 18 the individual correlation factors for each coolant are plotted against coolant temperatures according to equations (5c) and (6b), respectively, for cylinder A. For a given engine operating condition, coolant flow rate, and coolant temperature, the value of the

factor $\left[\frac{T_h - T_l}{W_c^{0.65}\,(T_g - T_h)} - 0.017\right] W_l^{0.6}$ or $\left[\frac{T_{b_o} - T_l}{W_c^{0.65}\left(T_g - T_{b_o}\right)}\right] W_l^{0.55}$

is indicative of the temperature difference between the cylinder walls and the coolant; the smaller its value the better the cooling quality of the coolant. Comparison of the separate curves for each coolant in figures 17 and 18 indicates the better cooling quality of water and the more aqueous solutions of ethylene glycol.

Equations (5c) and (6b) show that these correlation, or coolant-performance, factors are dependent upon the thermal conductivity, the specific heat, and the viscosity of the coolant. Substitution in equation (5c) of the values of the exponents and constant obtained for cylinder A (see equation (7)) results in

$$\left[\frac{T_h - T_l}{W_c^{0.65}\,(T_g - T_h)} - 0.017\right] W_l^{0.6} = 0.00418\,\frac{\mu^{0.2}}{c^{0.4}\,k^{0.6}} \qquad (11)$$

Thus, it is evident that high thermal conductivity and specific heat and low viscosity are desirable from forced-convection cooling considerations and that, for a given percentage change in these properties, the cooling is affected most by the change in thermal conductivity, somewhat less by the change in specific heat, and only slightly by the change in viscosity. The relative magnitude of the effects of these properties as indicated by the exponents of equation (11) may, of course, be expected to vary somewhat with different engines.

CONCLUSIONS

For the ranges of conditions investigated in previously reported tests conducted with two liquid-cooled cylinders using water and aqueous ethylene-glycol solutions as coolants it has been found that:

1. The expressions derived from an analysis based on forced-convection heat-transfer theory of the cooling processes in liquid-cooled engine cylinders provide satisfactory methods of correlating the average head and barrel temperatures with the primary engine and coolant variables.

2. The equations obtained for the cylinder head and barrel temperatures as a function of the engine operating conditions and the flow rate, the temperature, and the physical properties of the coolants represent the test data with good accuracy.

3. The physical properties of the coolant appearing in these equations in order of their importance in determining the heat-transfer quality of the coolants are the thermal conductivity, the specific heat, and the viscosity. The cooling performance of the various coolants investigated is adequately correlated by these physical properties in the correlation equation.

Aircraft Engine Research Laboratory,
National Advisory Committee for Aeronautics,
Cleveland, Ohio.

REFERENCES

1. Pinkel, Benjamin: Heat-Transfer Processes in Air-Cooled Engine Cylinders. NACA Rep. No. 612, 1938.

2. Pinkel, Benjamin, and Ellerbrock, Herman H., Jr.: Correlation of Cooling Data from an Air-Cooled Cylinder and Several Multi-cylinder Engines. NACA Rep. No. 683, 1940.

3. Manganiello, Eugene J., and Bernardo, Everett: Cylinder Temperatures of Two Liquid-Cooled Aircraft Cylinders for Various Engine and Coolant Conditions. NACA ARR No. E5H13, 1945.

4. Cragoe, C. S.: Properties of Ethylene Glycol and Its Aqueous Solutions. Cooperative Fuel Res. Committee, CRC, July 1943.

5. Bernardo, Everett, and Eian, Carroll S.: Heat-Transfer Tests of Aqueous Ethylene Glycol Solutions in an Electrically Heated Tube. NACA ARR No. E5F07, 1945.

6. Ellerbrock, Herman H., Jr., and Rollin, Vern G.: Correlation of Single-Cylinder Cooling Tests of a Pratt & Whitney R-2800-21 Engine Cylinder with Wind Tunnel Tests of a Pratt & Whitney R-2800-27 Engine. NACA ARR No. 3L14, 1943.

7. McAdams, William H.: Heat Transmission. McGraw-Hill Book Co., Inc., 2d ed., 1942, p. 168.

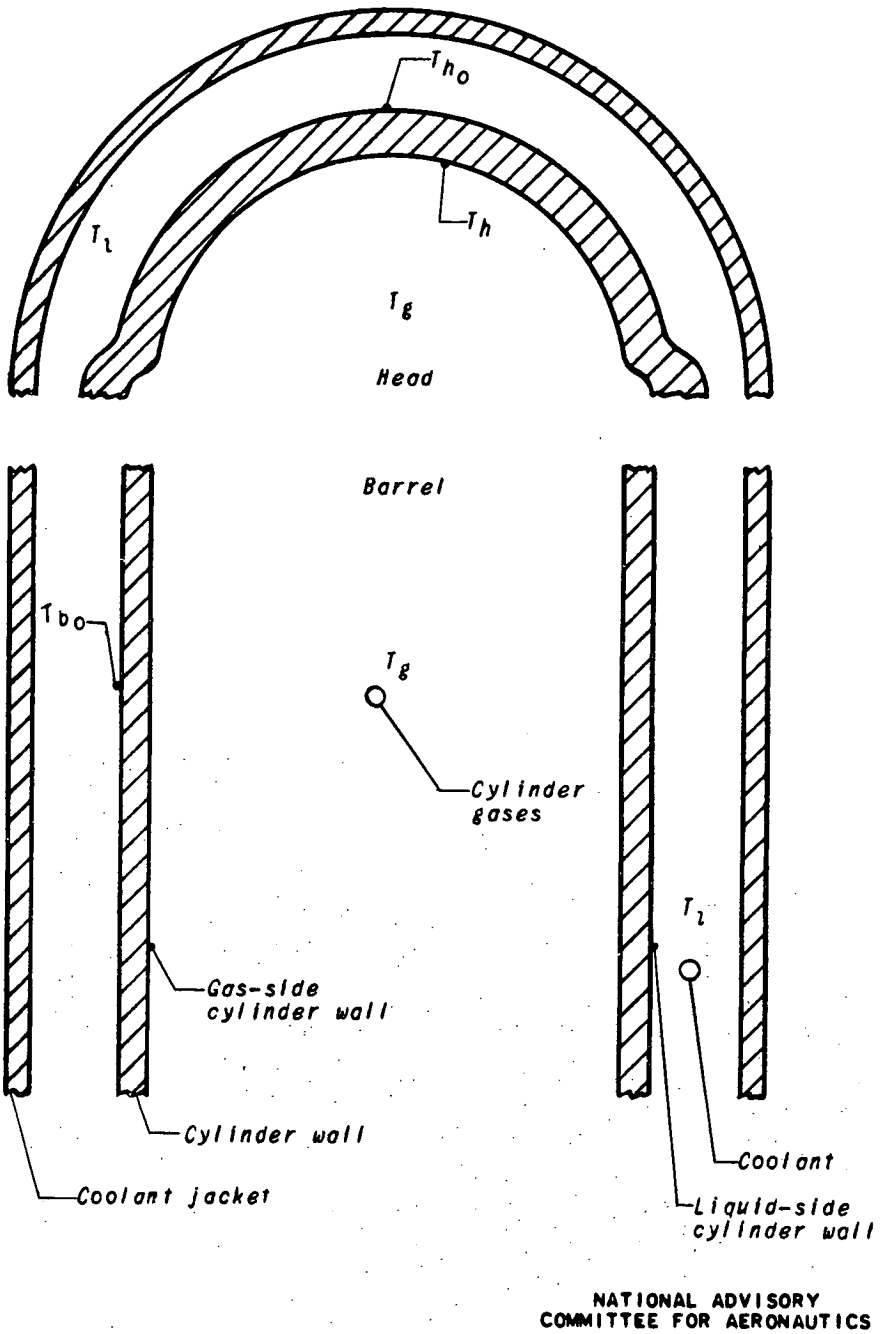

Figure 1. - Diagrammatic sketch of a liquid-cooled engine cylinder illustrating the various sections.

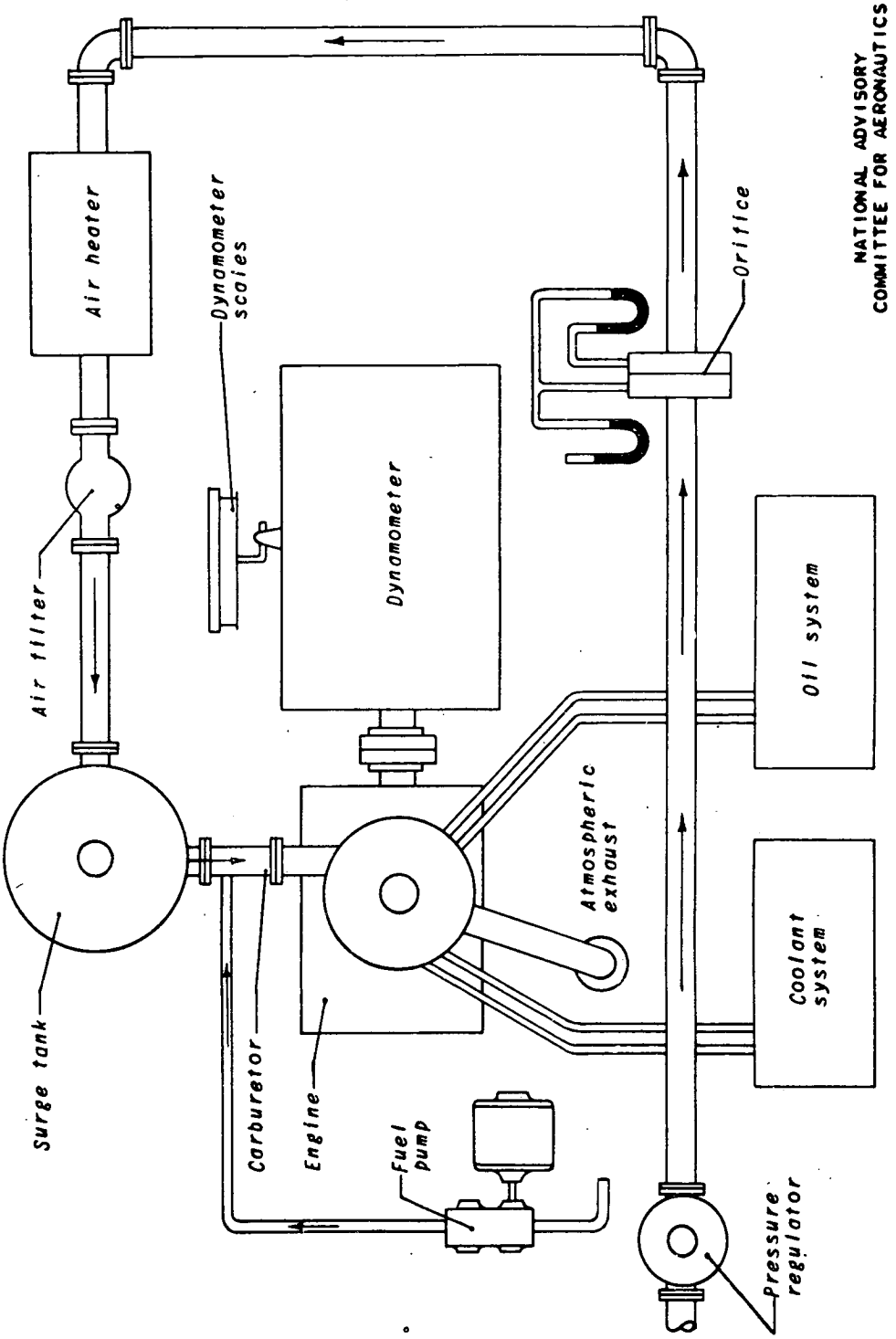

Figure 2. - Diagrammatic layout of engine-testing setup.

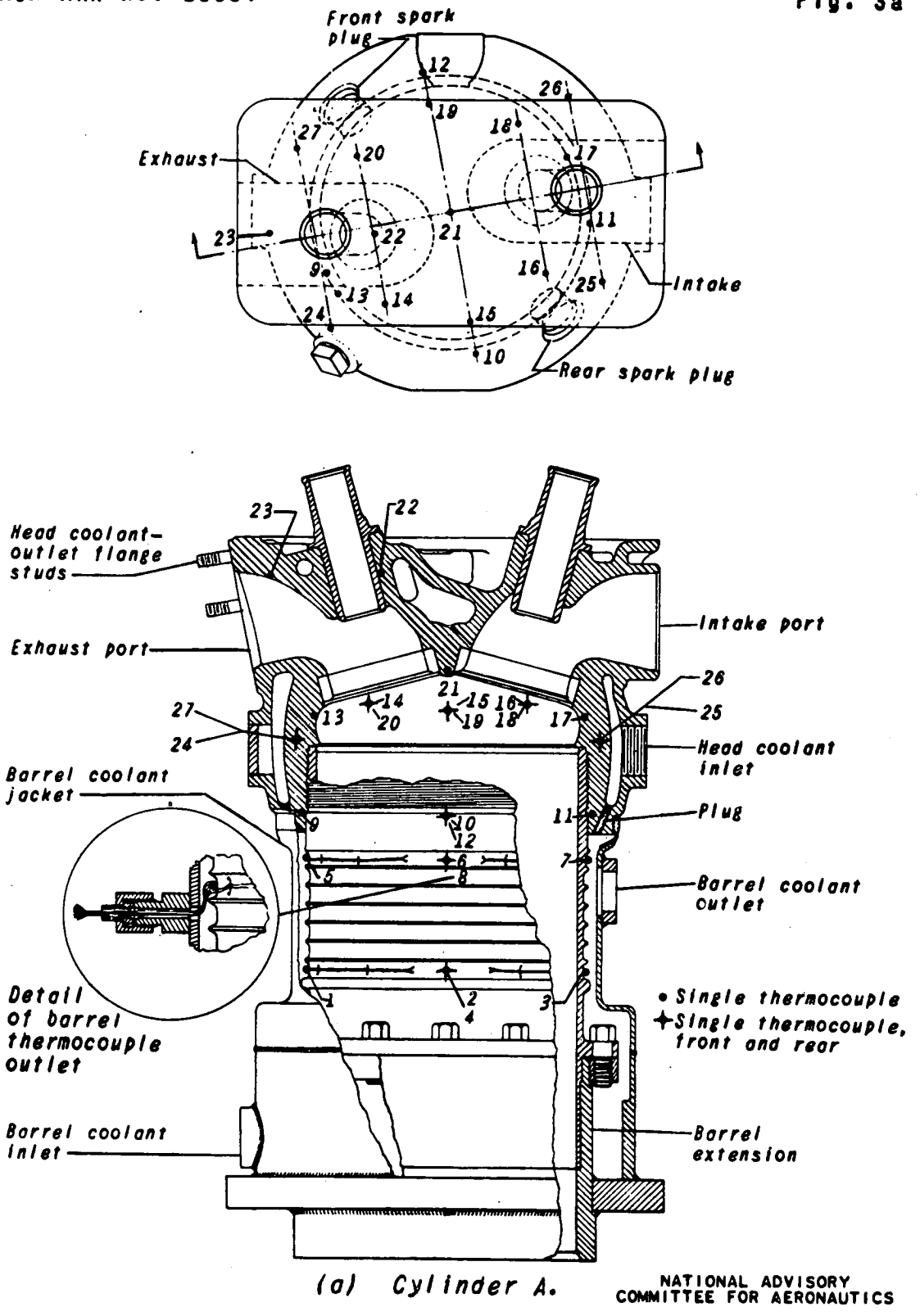

Figure 3. - Thermocouple installation and details of cylinders A and B.

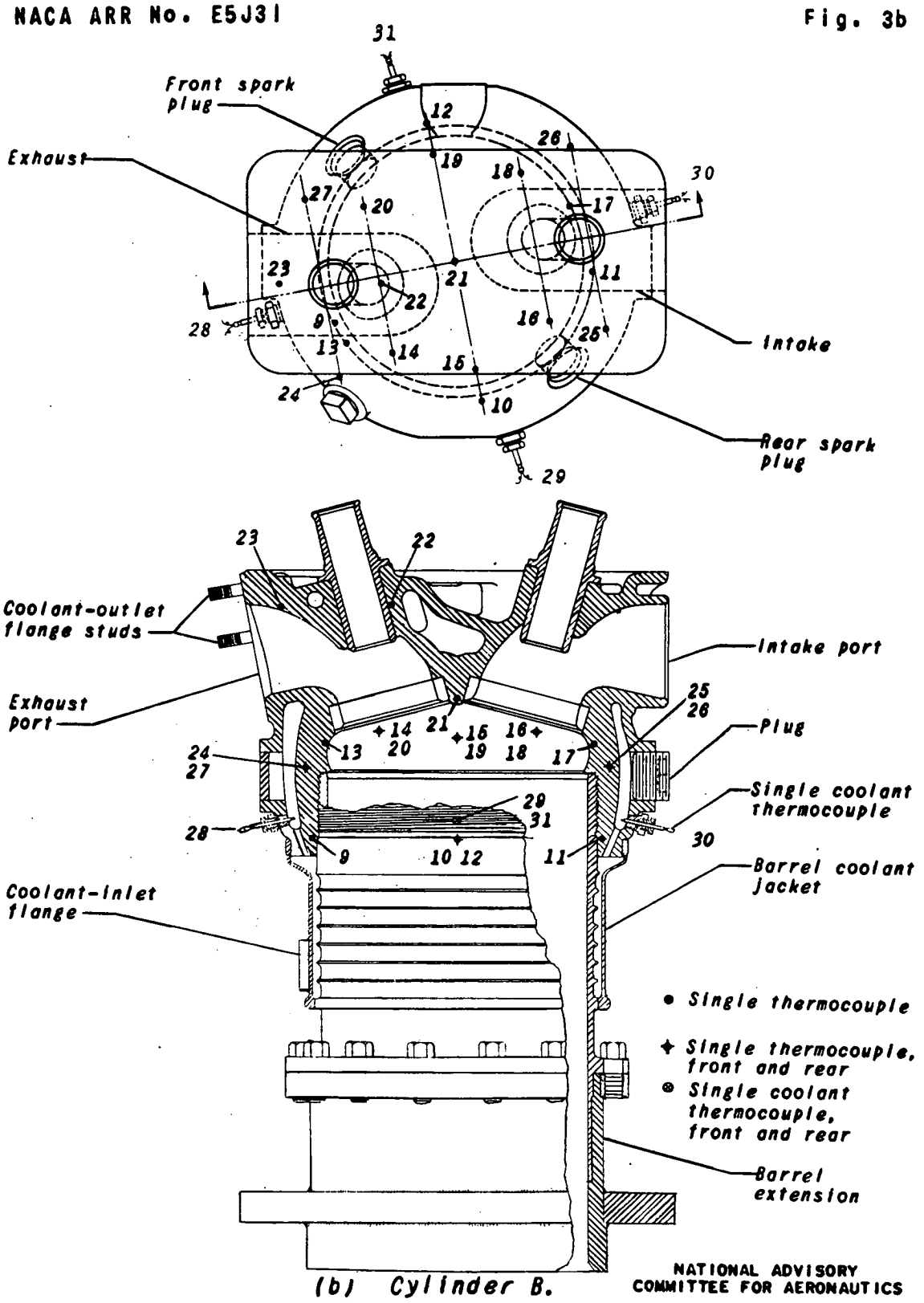

(b) Cylinder B.

Figure 3. - Concluded.

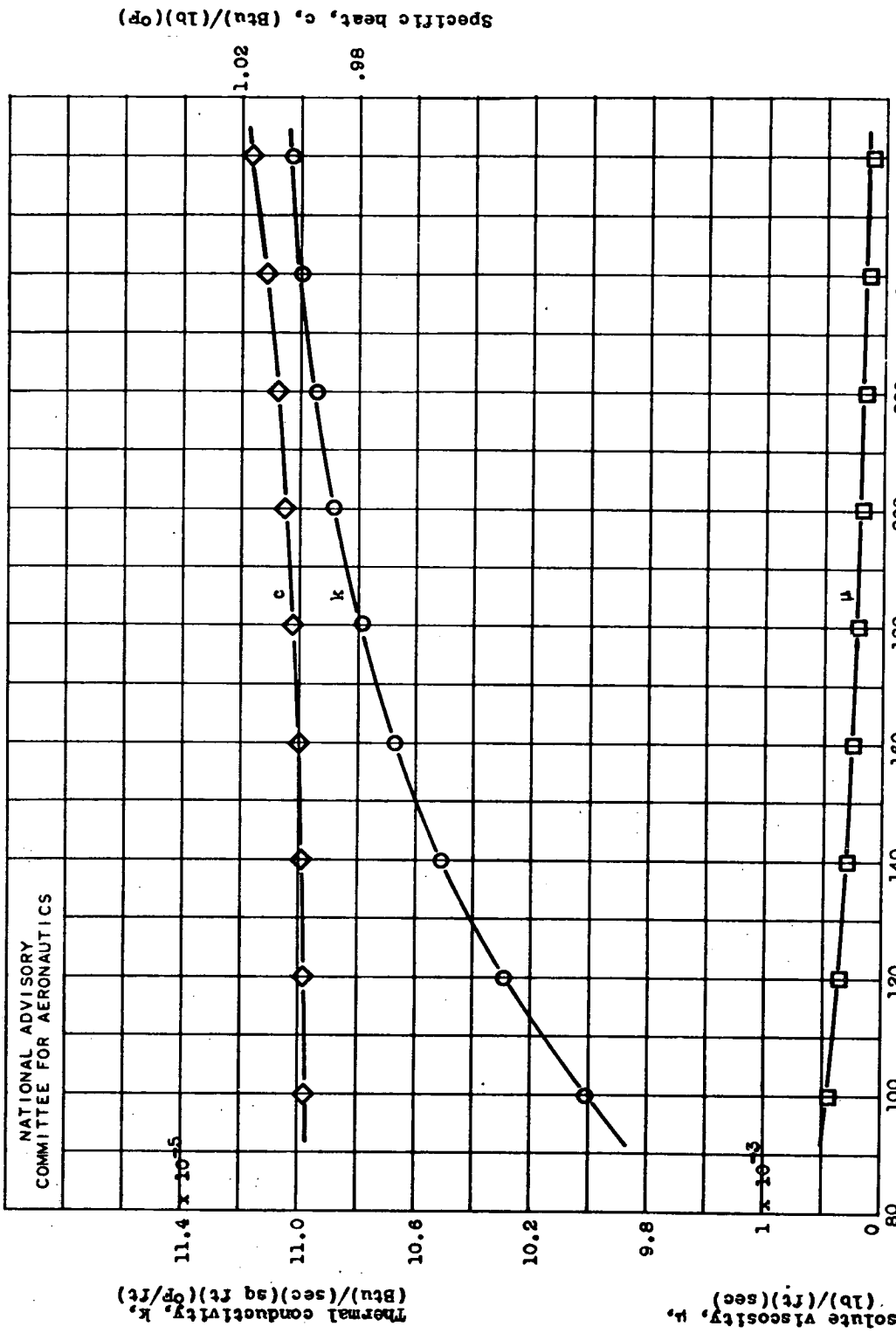

Figure 4.- Variation of thermal conductivity, specific heat, and viscosity of water with temperature. (Data from reference 4.)

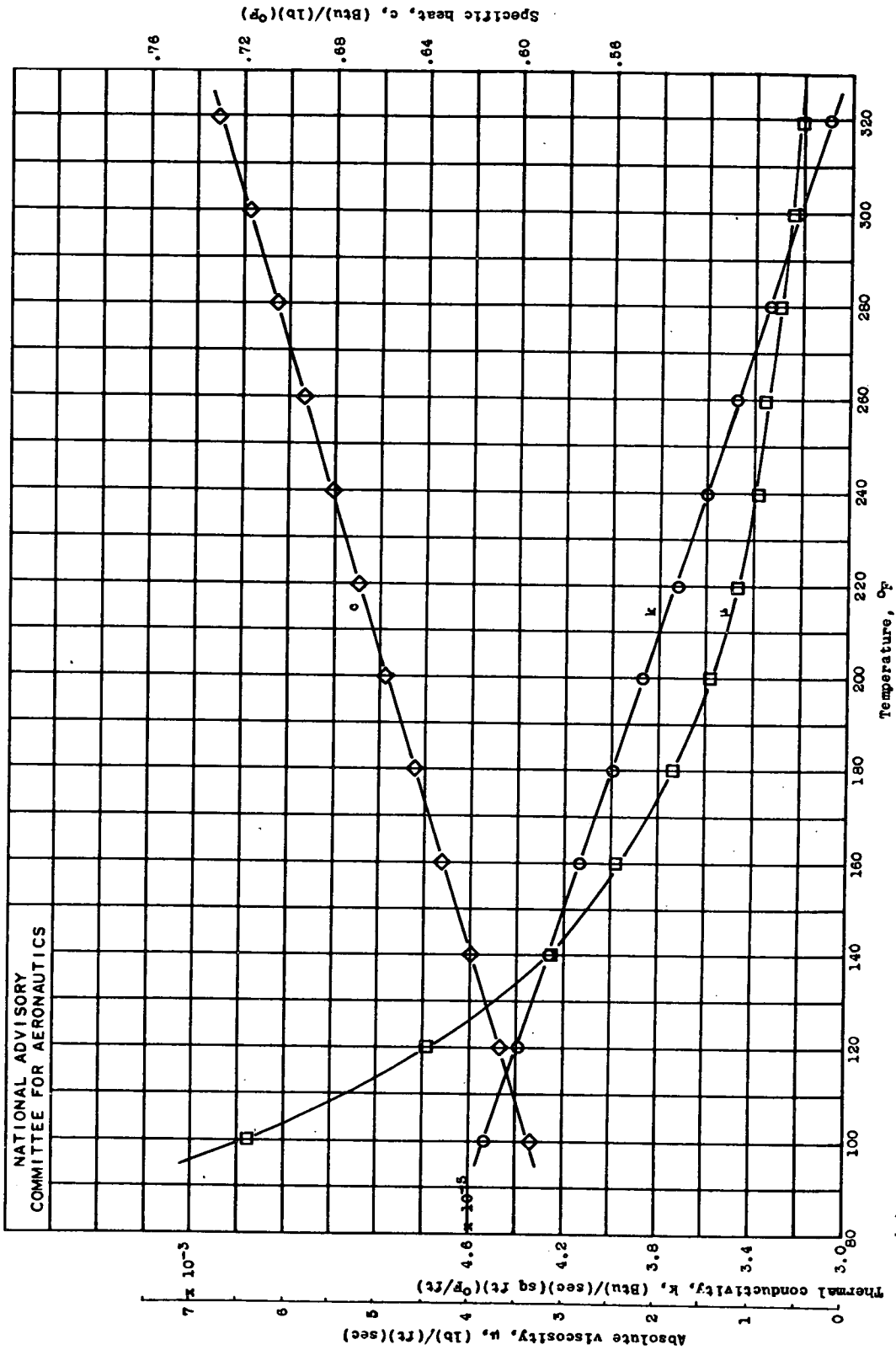

(a) 97 percent-3 percent (by volume) glycol-water solution.

Figure 5.- Variation of thermal conductivity, specific heat, and viscosity of aqueous ethylene-glycol solutions with temperature. (Data from reference 4.)

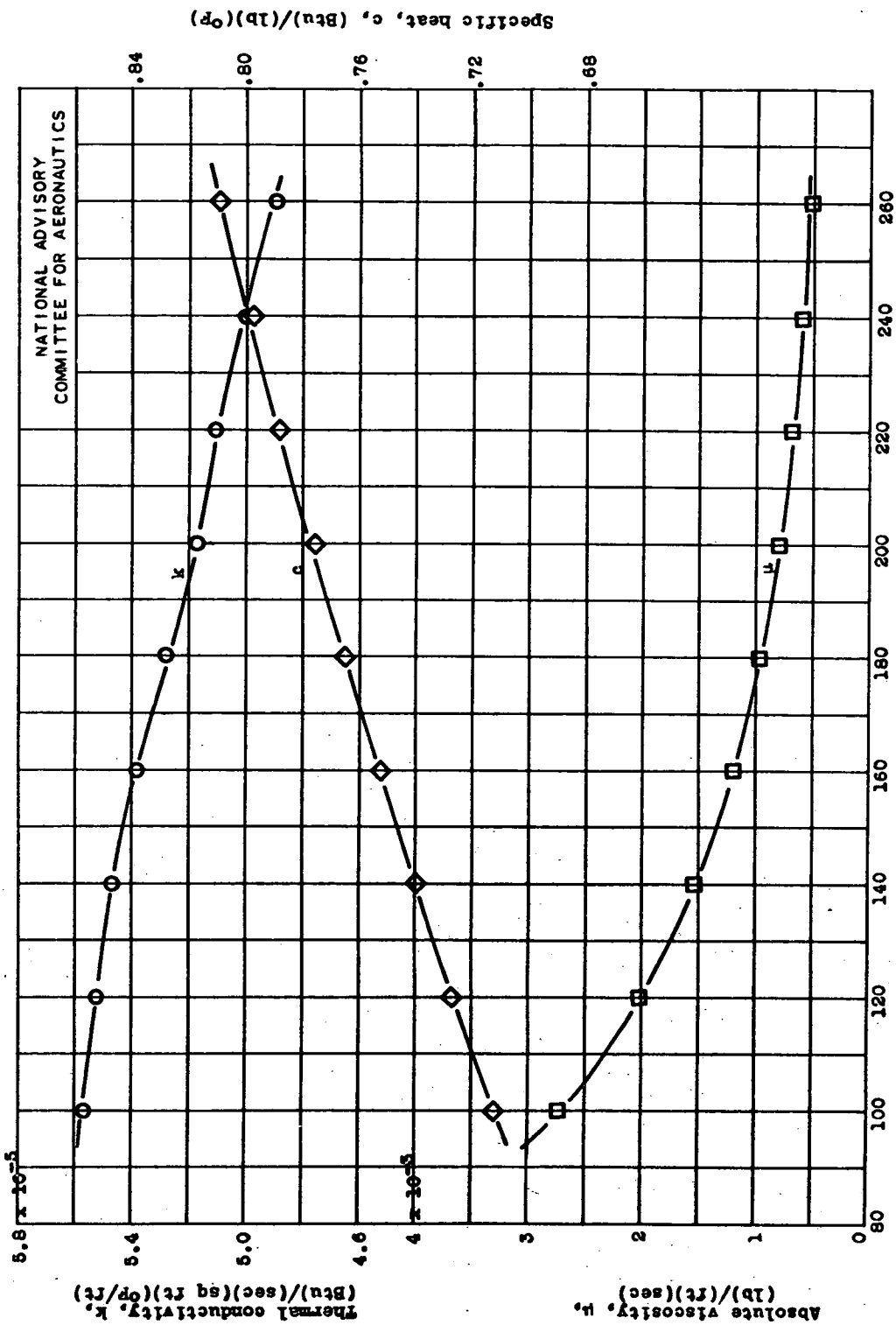

(b) 70 percent-30 percent (by volume) glycol-water solution.

Figure 5.- Continued.

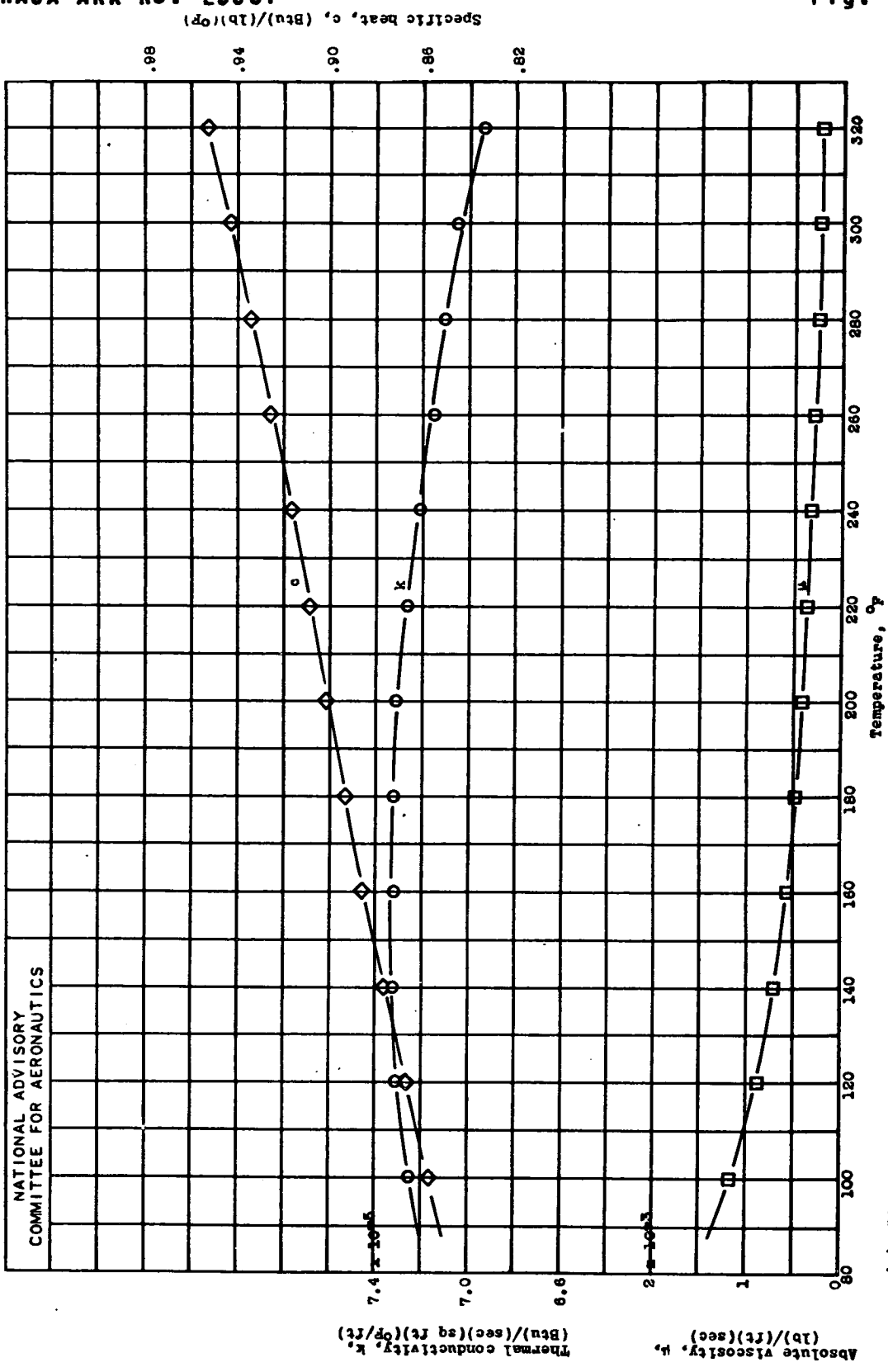

(c) 38 percent-62 percent (by volume) glycol-water solution.

Figure 5. Continued.

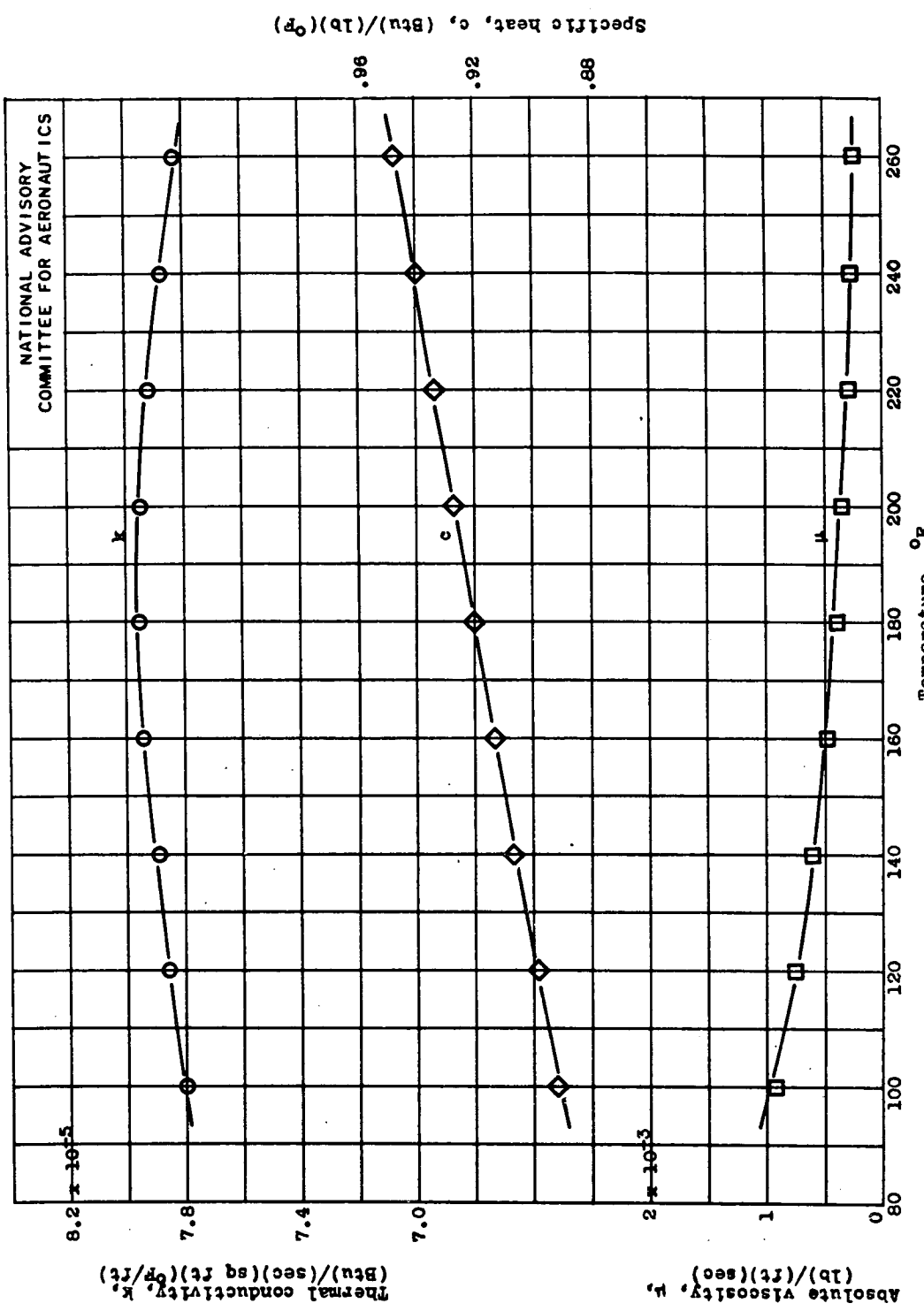

(d) 30 percent-70 percent (by volume) glycol-water solution.

Figure 5.- Concluded.

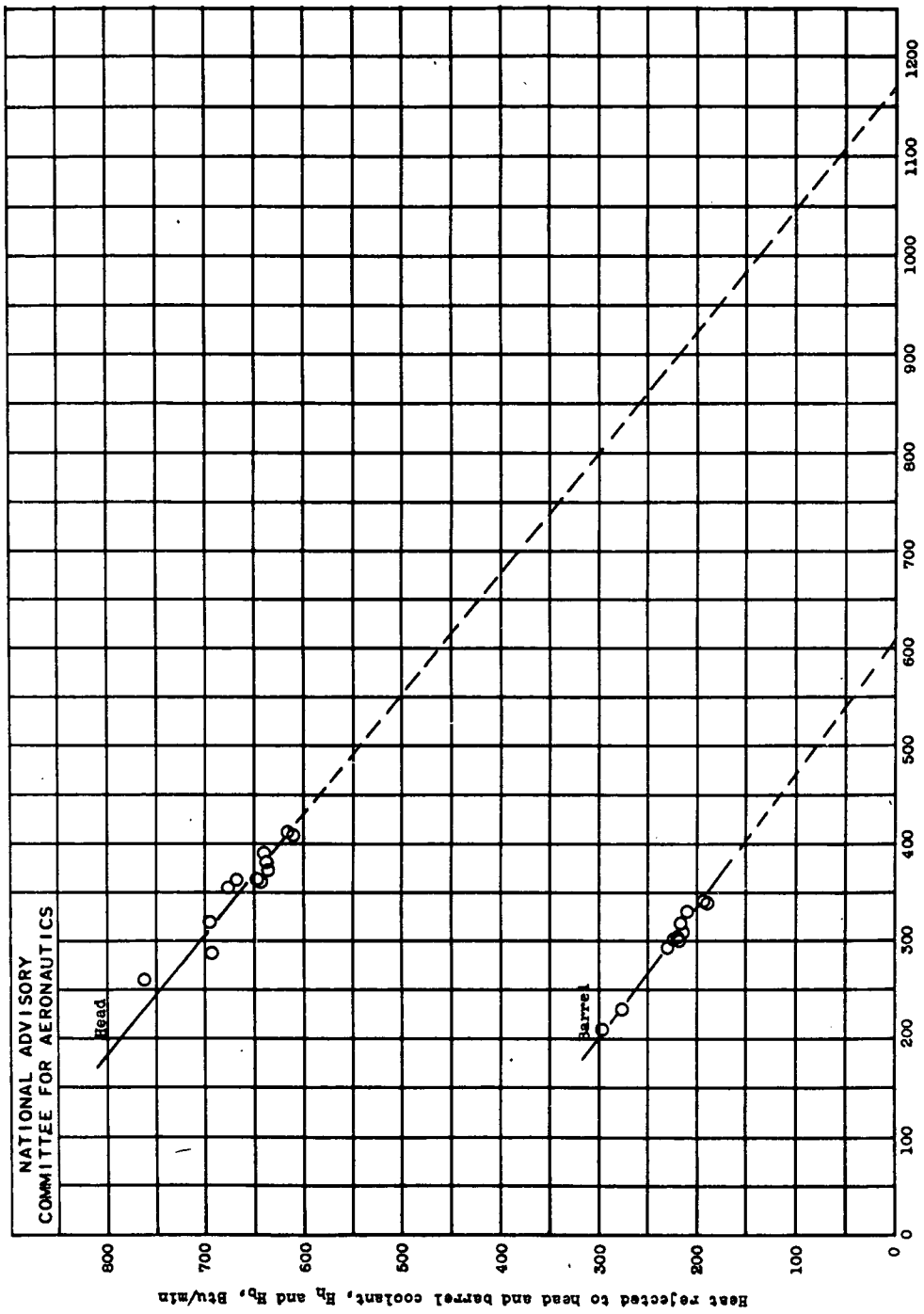

Figure 6.- Determination of T_g from the variation of heat rejected to head and barrel coolant with average head and barrel temperatures. Cylinder A, coolant, AN-E-2 ethylene glycol; average coolant temperature: head, 125° F to 293° F, barrel, 126° F to 311° F; coolant flow rate: head, 49 to 135 pounds per minute, barrel, 15 to 47 pounds per minute; engine speed, 2000 rpm; charge flow rate, 5.4 pounds per minute, fuel-air ratio, 0.077; spark advance, 28° B.T.C.; carburetor-air temperature, 80° F.

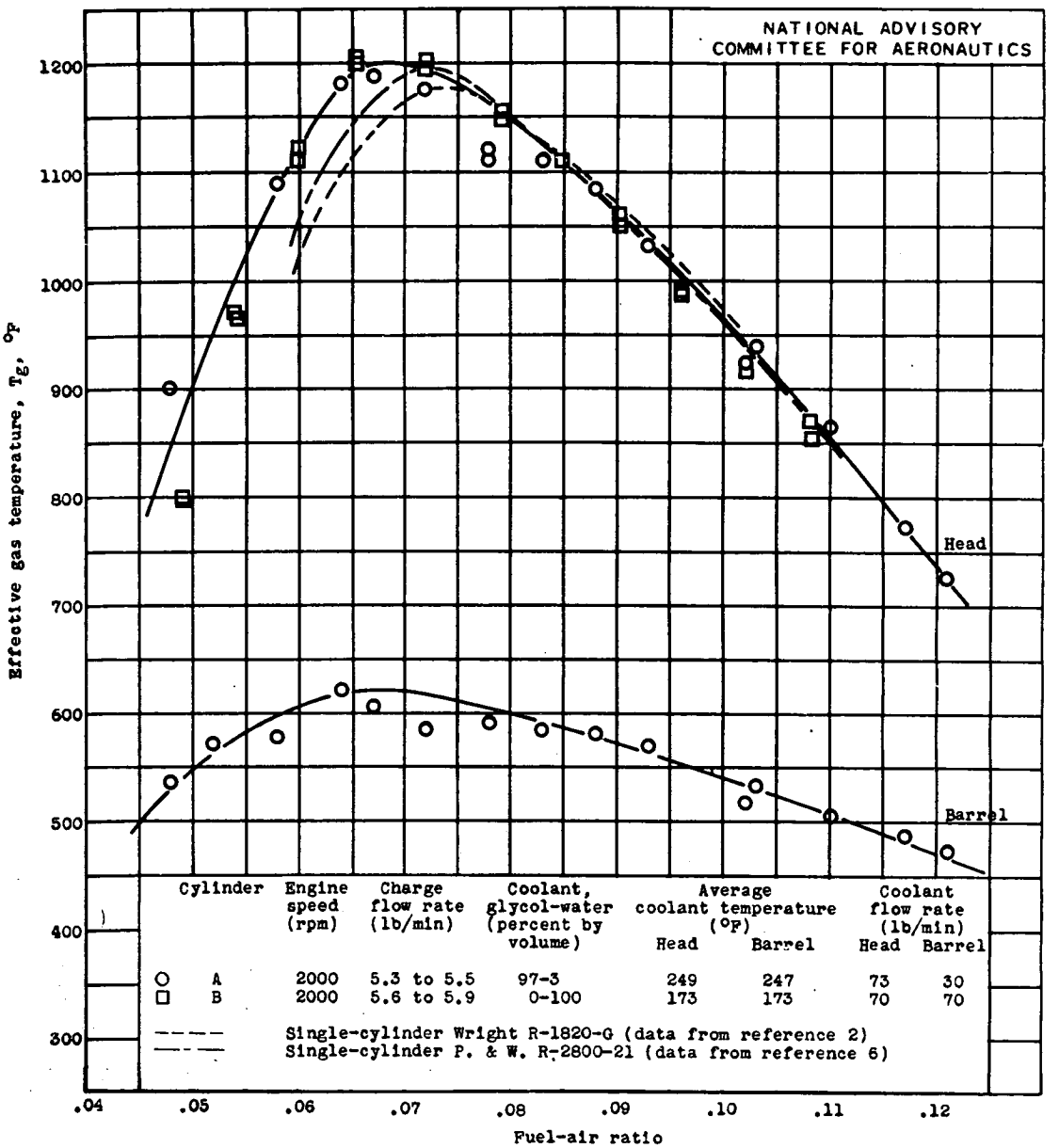

Figure 7.- Variation of effective gas temperature with fuel-air ratio for the head and barrel. Spark advance, 28° B.T.C.; carburetor-air temperature, 80° F.

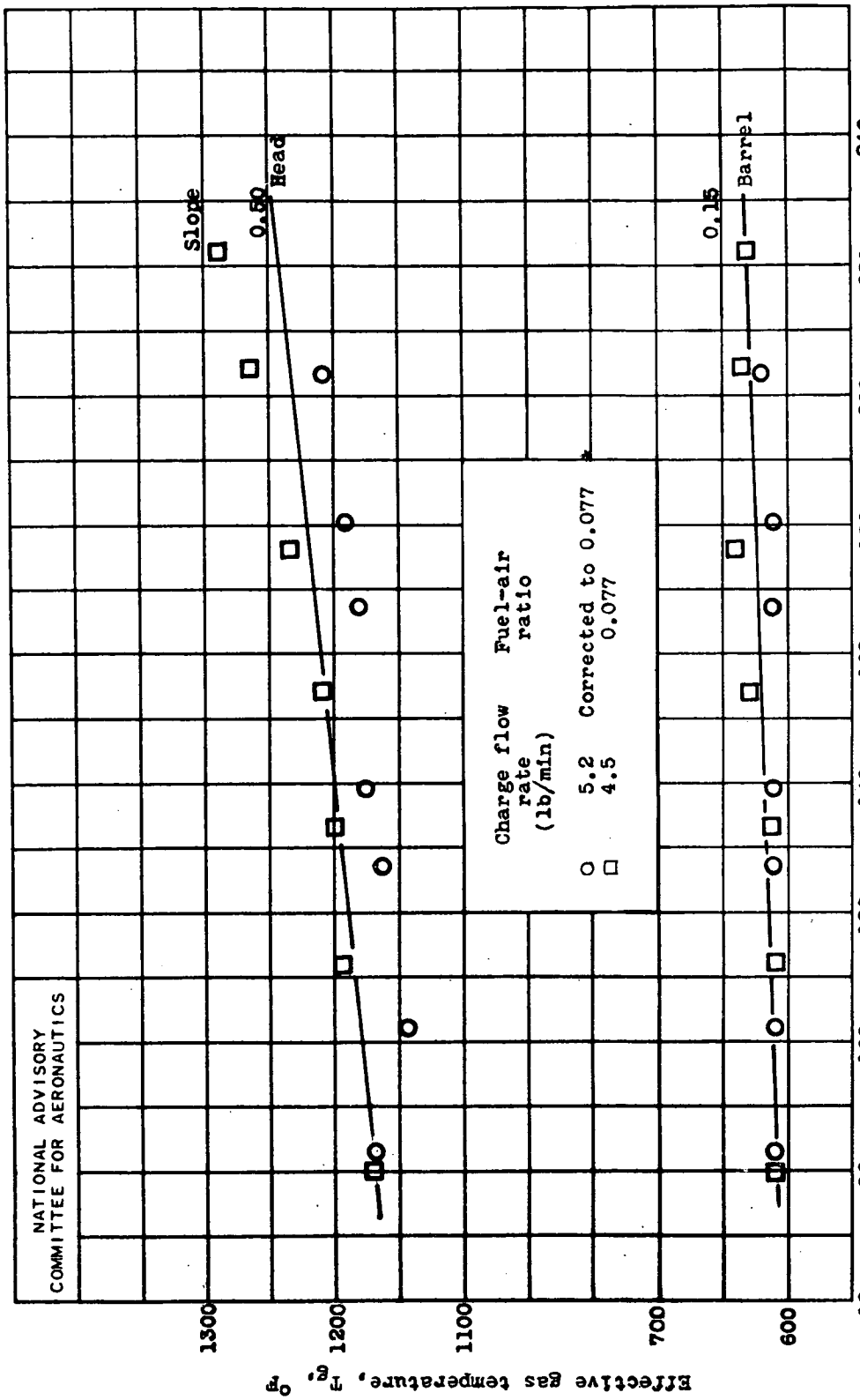

Figure 8.- Variation of effective gas temperature with carburetor-air temperature for the head and barrel. Cylinder A; coolant, AN-E-2 ethylene glycol; average coolant temperature: head, 249° F, barrel, 247° F; coolant flow rate: head, 72 pounds per minute, barrel, 30 pounds per minute; engine speed, 2000 rpm; spark advance, 28° B.T.C.

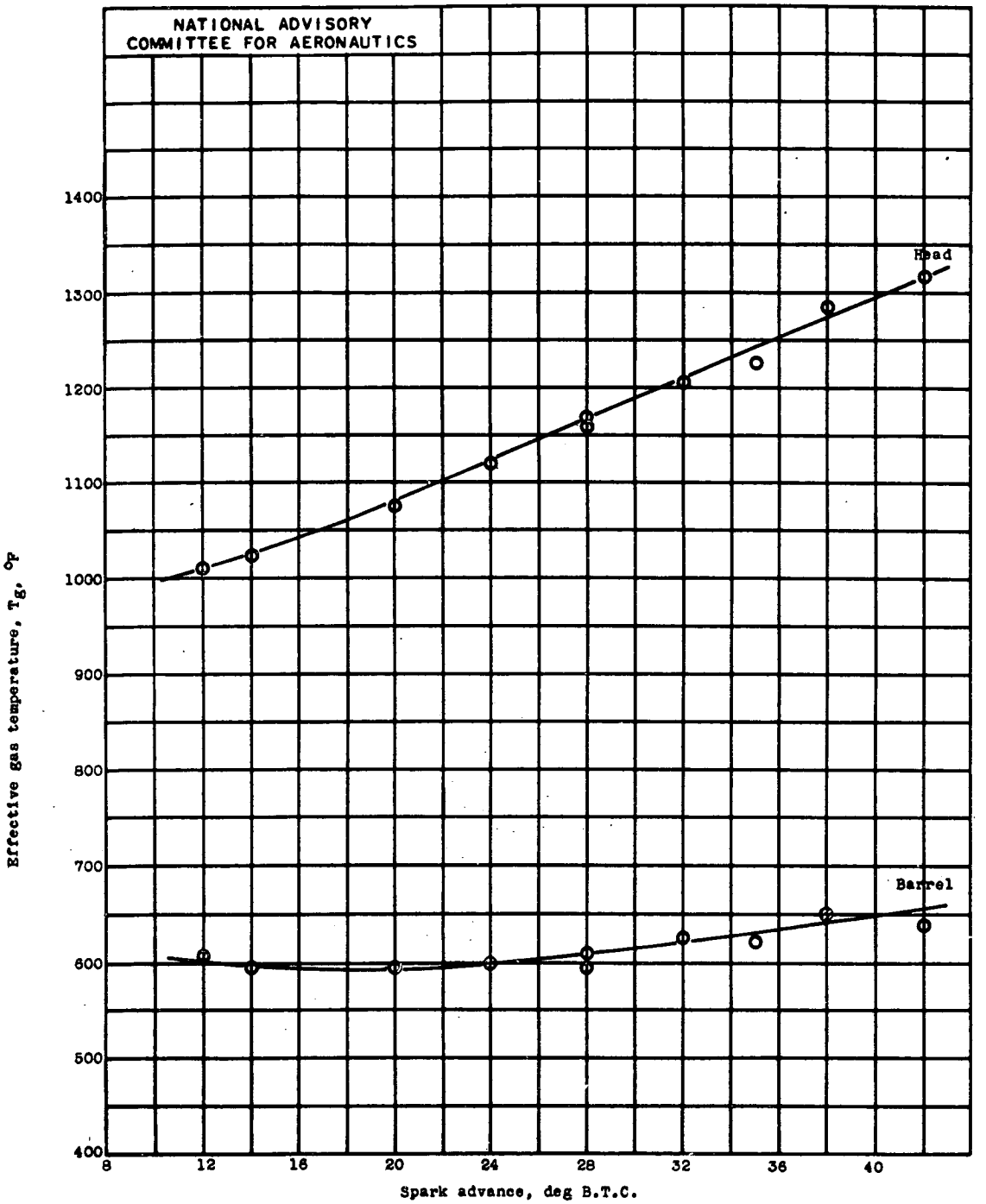

Figure 9.- Variation of effective gas temperature with spark advance for the head and barrel. Cylinder A; coolant, AN-E-2 ethylene glycol; average coolant temperature: head, 249° F, barrel, 247° F; coolant flow rate: head, 72 pounds per minute, barrel, 30 pounds per minute; engine speed, 2000 rpm; charge flow rate, 5.4 pounds per minute; fuel-air ratio, 0.077; carburetor-air temperature, 83° F.

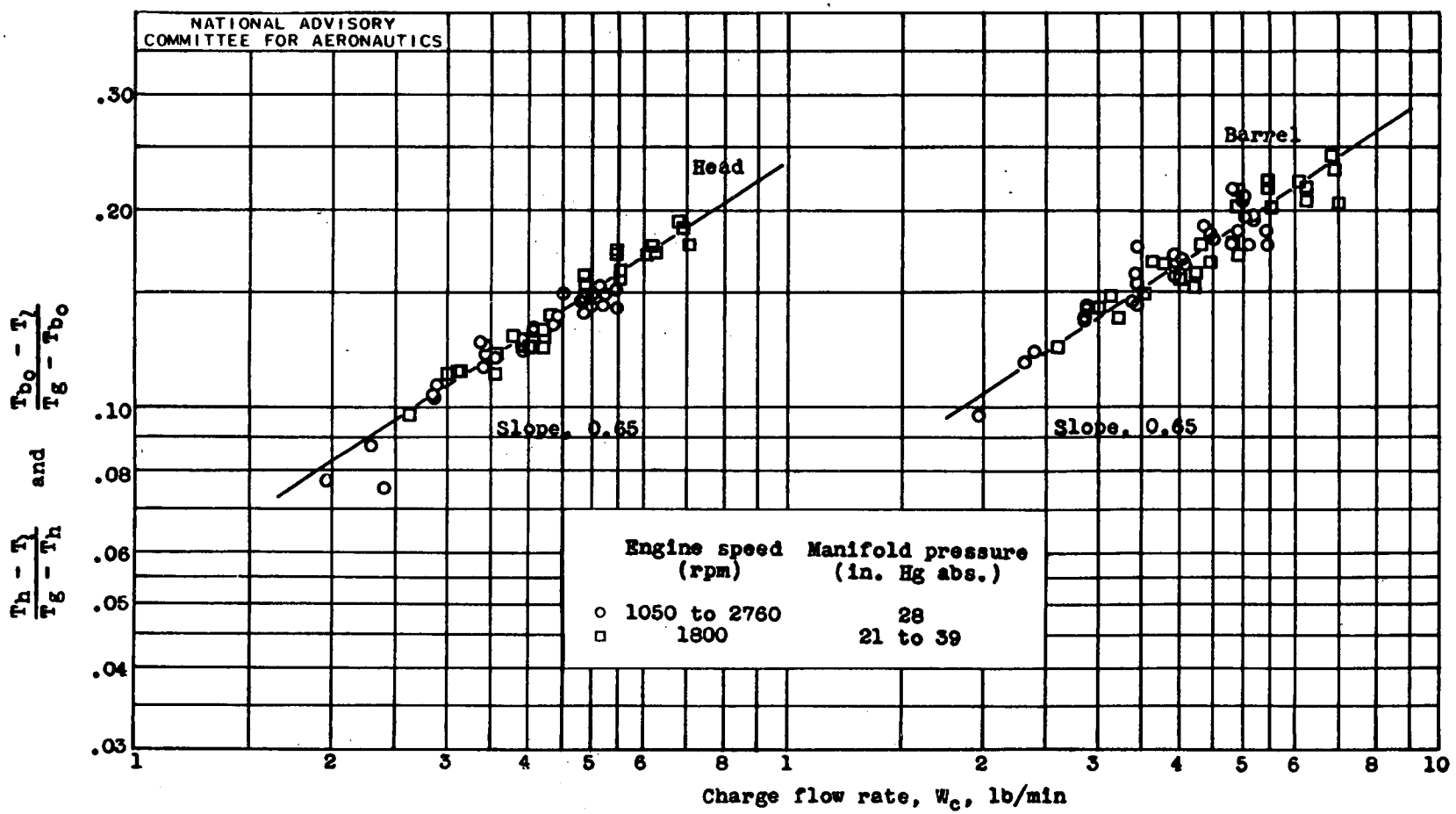

Figure 10.- Determination of exponents of charge flow rate from the variation of $(T_h - T_l)/(T_g - T_h)$ and $(T_{b_o} - T_l)/(T_g - T_{b_o})$ with W_c. Cylinder A; coolant, AN-E-2 ethylene glycol; average coolant temperature, 247° F; coolant flow rate: head, 73 pounds per minute, barrel, 30 pounds per minute; fuel-air ratio, 0.077; spark advance, 28° B.T.C.; carburetor-air temperature, 80° F.

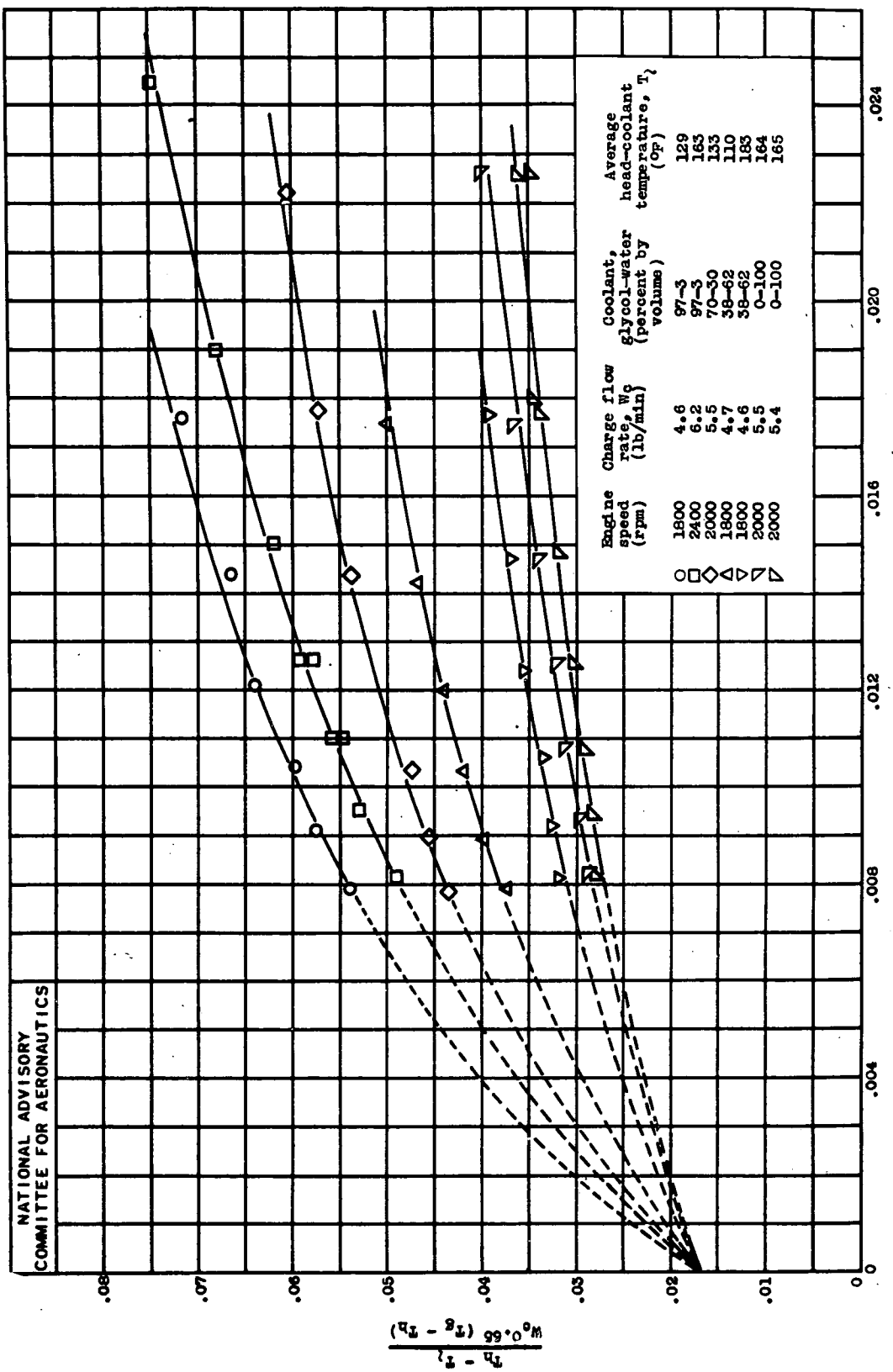

Figure 11.- Determination of the factor Z from the variation of $(T_h - T_l)/W_c^{0.65}(T_g - T_h)$ with $1/W_l$. Cylinder 4; fuel-air ratio, 0.077; spark advance, 28° B.T.C.; carburetor-air temperature, 82° F.

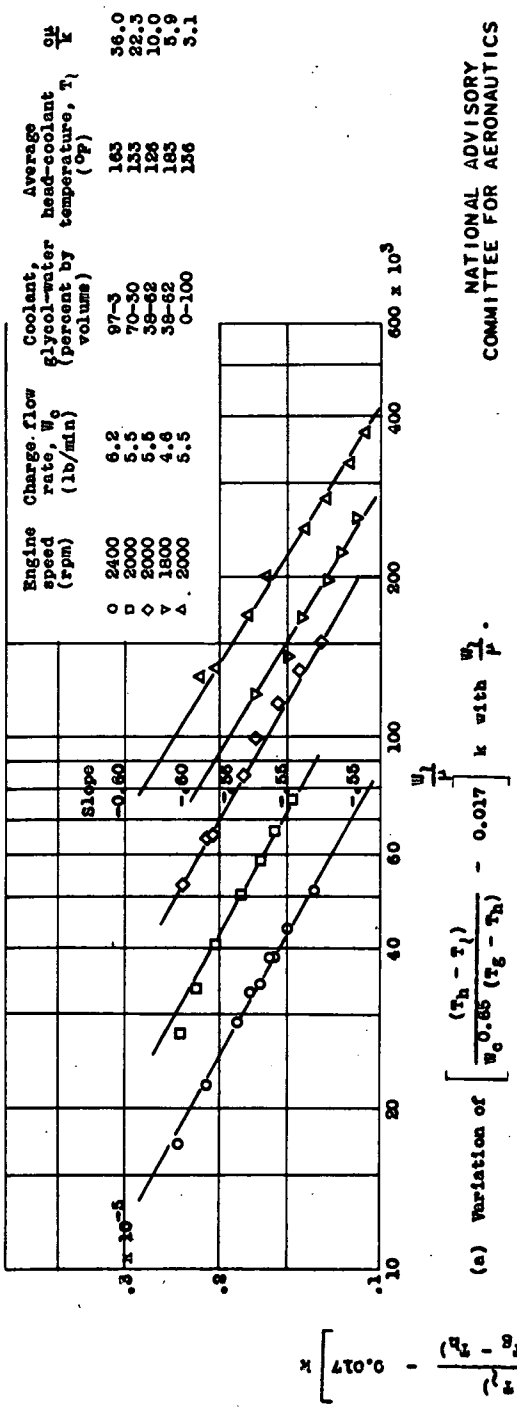

Figure 12.- Determination of the exponent of $\frac{c\mu}{k}$. Cylinder 4; fuel-air ratio, 0.077; spark advance, 28° B.T.C.; carburetor-air temperature, 82° F.

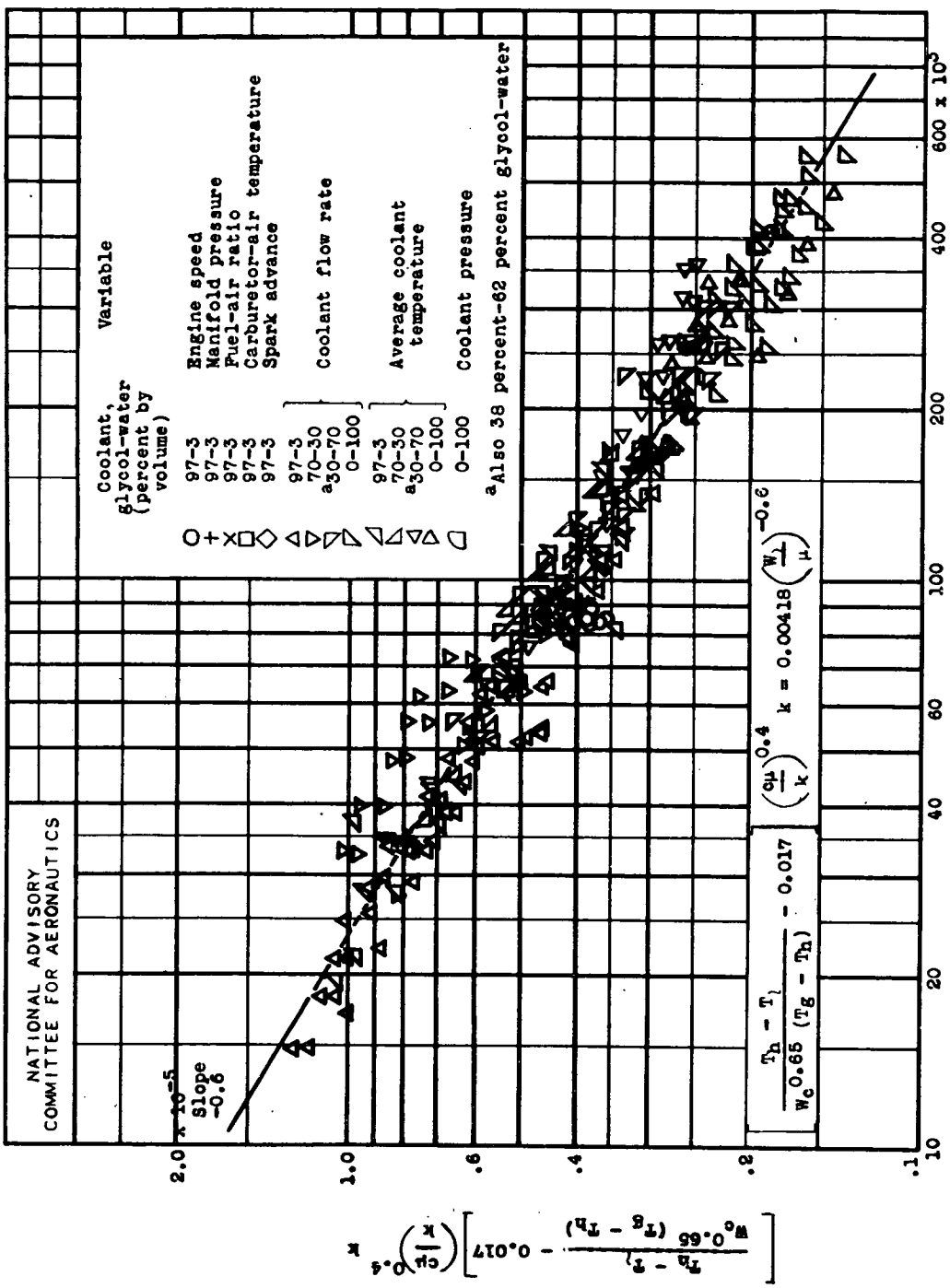

Figure 13.- Final correlation of average gas-side head temperatures for cylinder A.

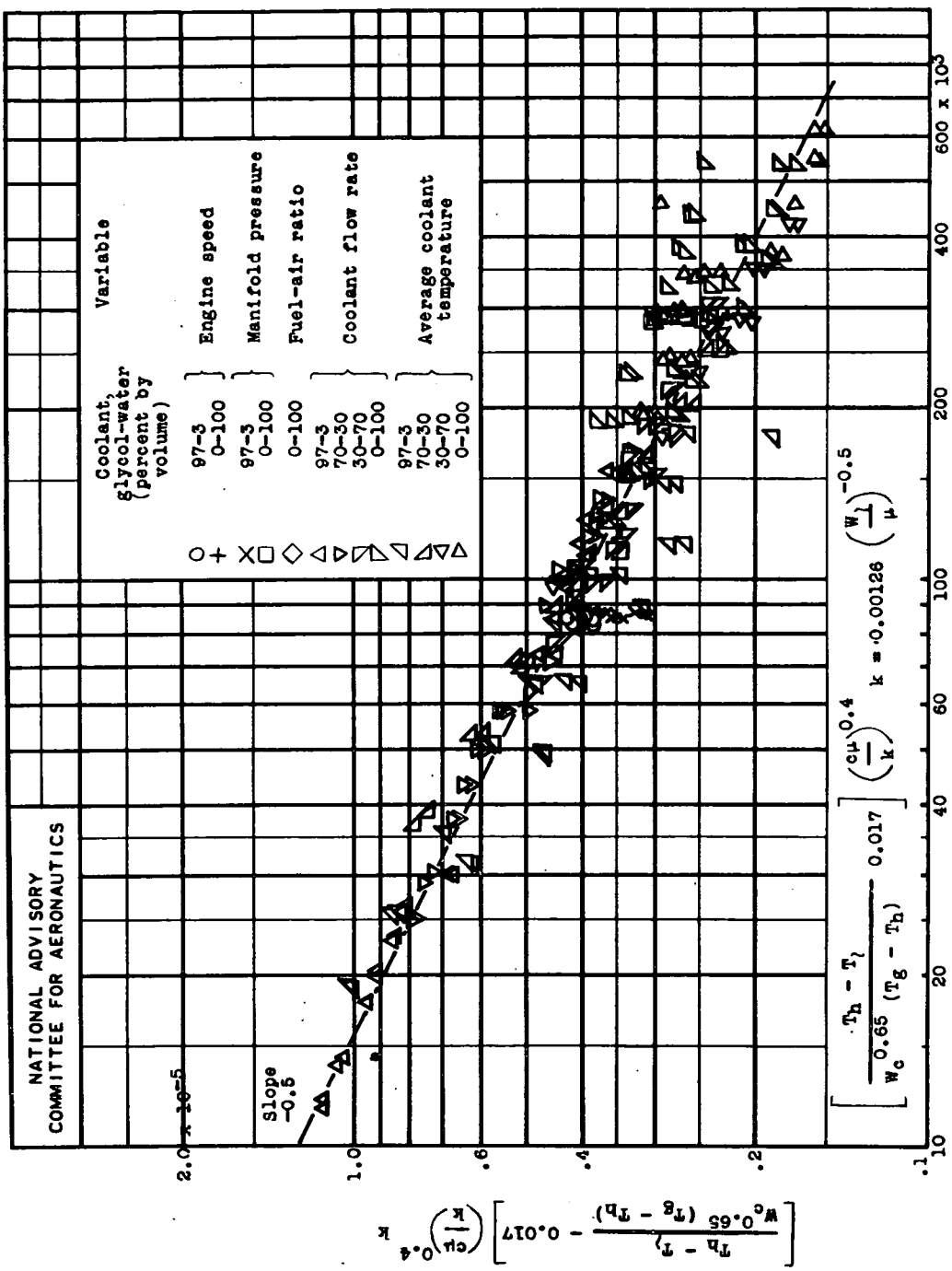

Figure 14.- Final correlation of average gas-side head temperatures for cylinder B.

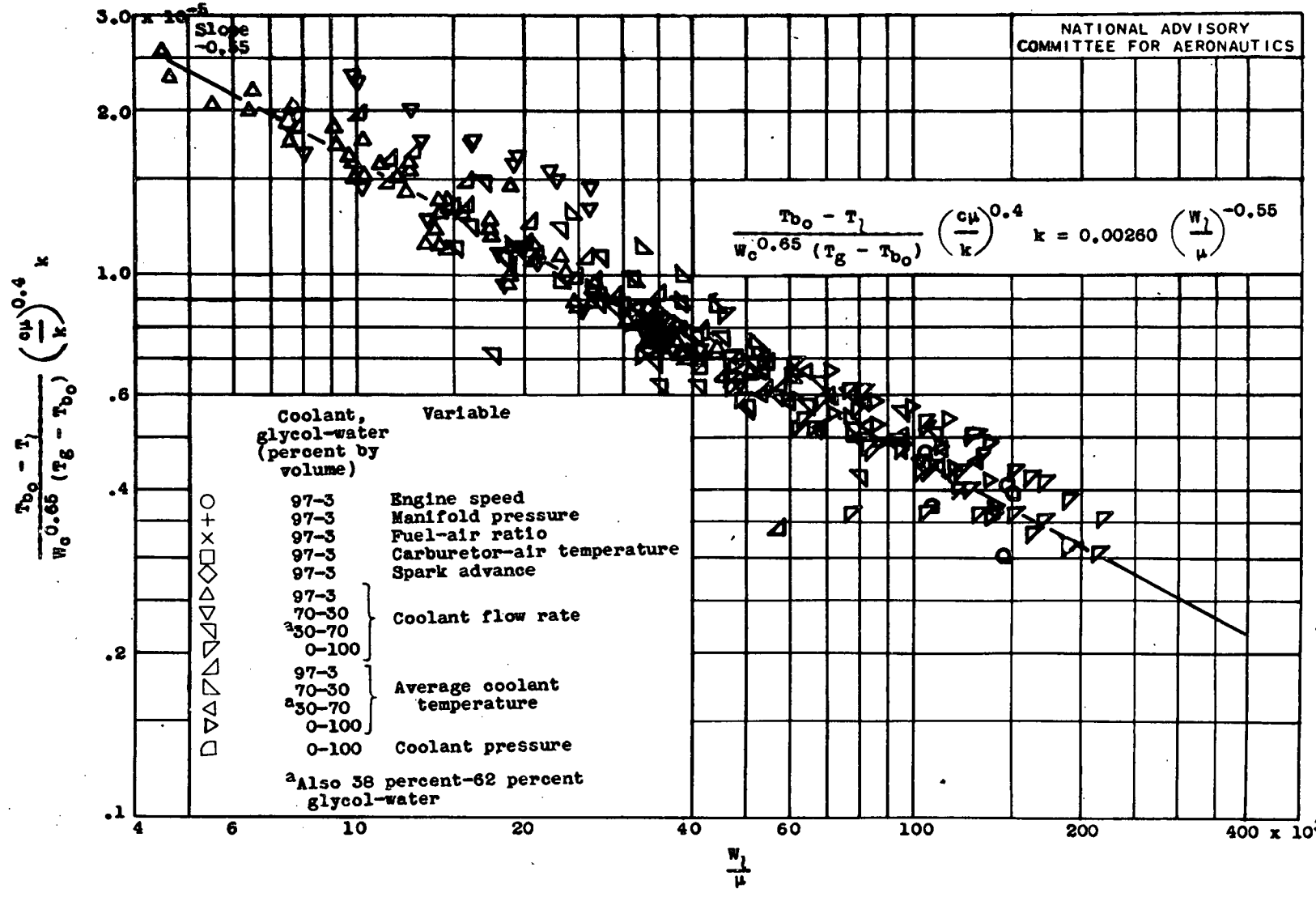

Figure 15.- Final correlation of average liquid-side barrel temperatures for cylinder A.

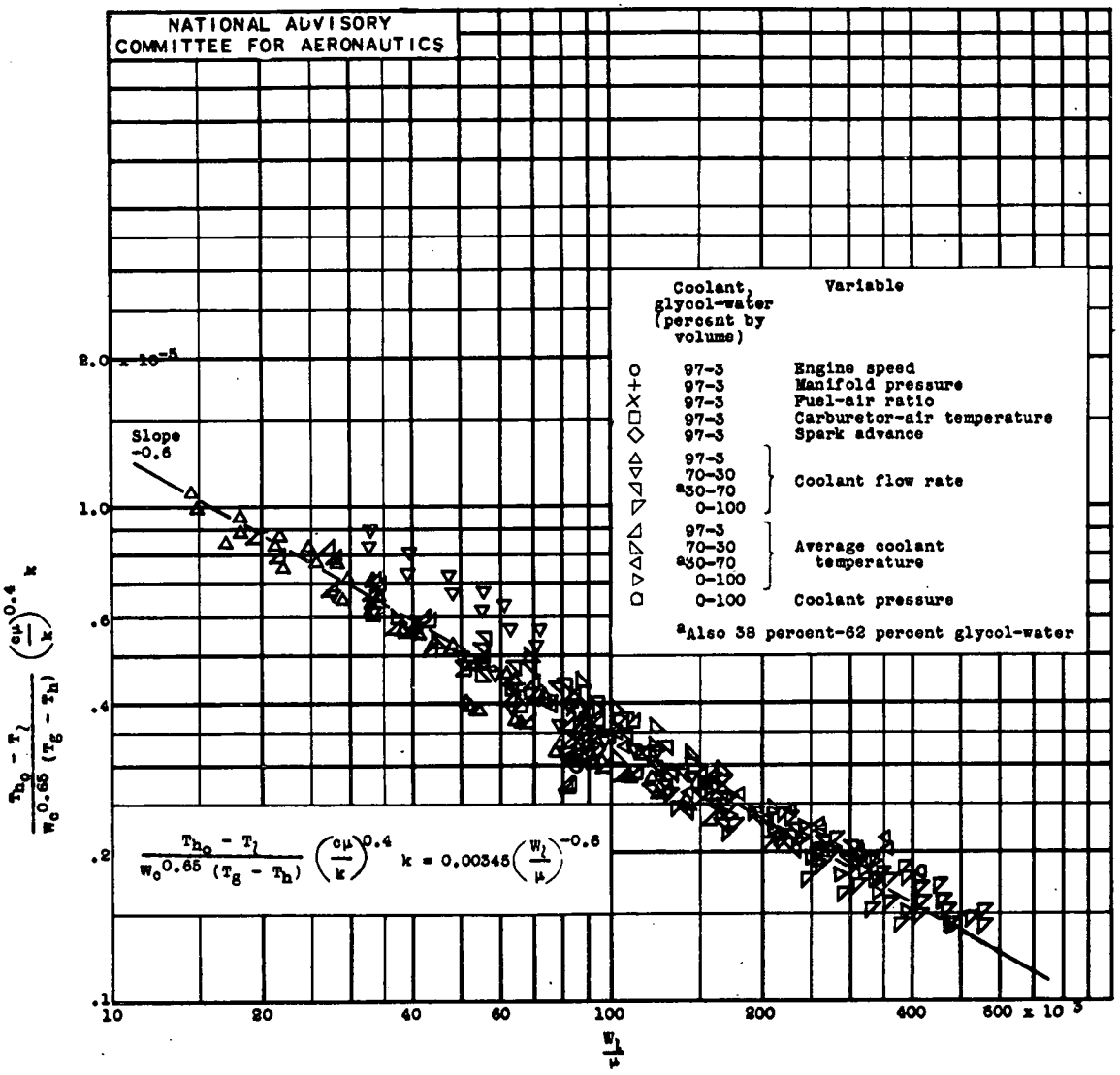

Figure 16.- Final correlation of average head temperatures for cylinder A on the basis of T_h and T_{h_o}.

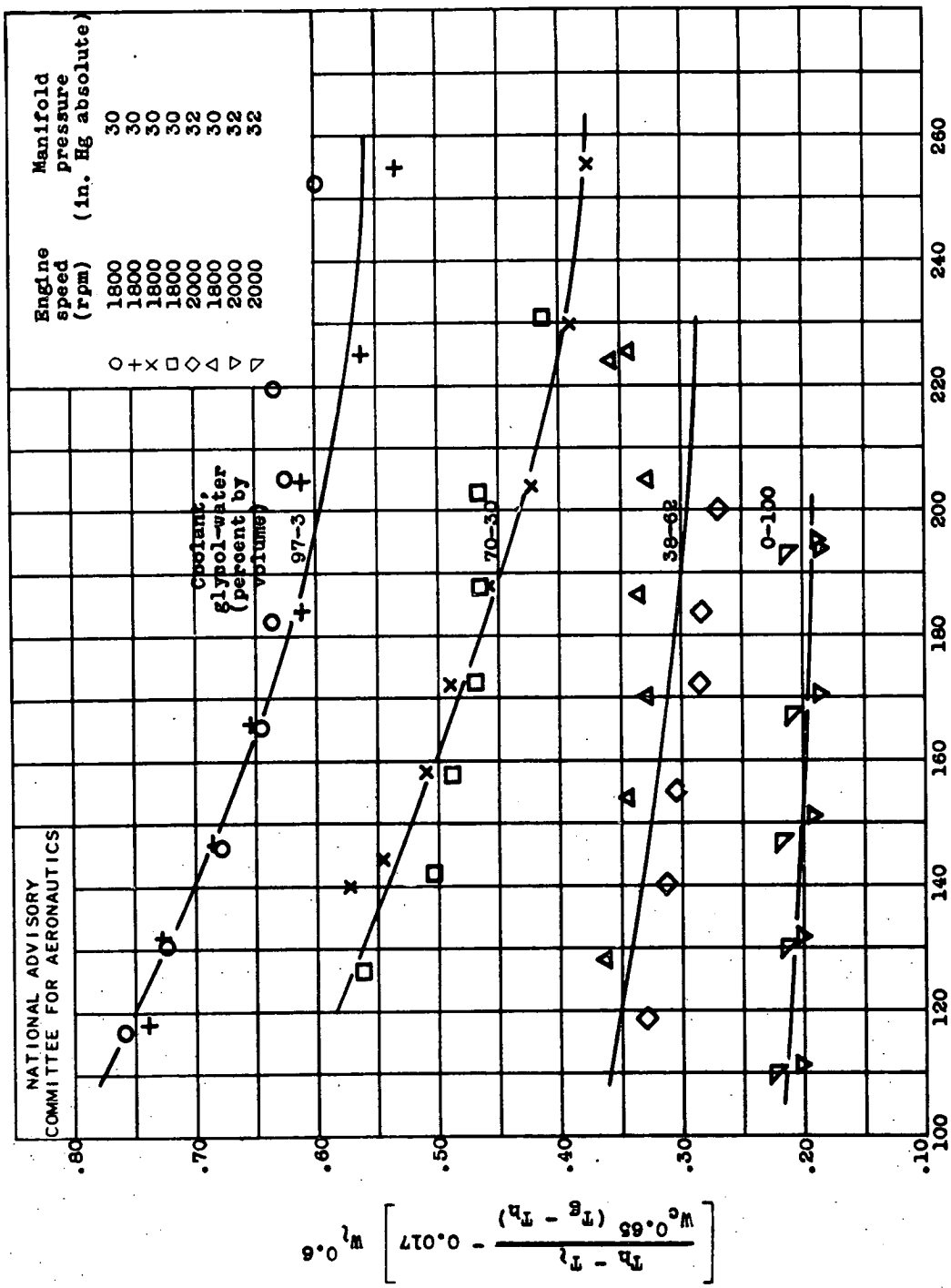

Figure 17.- Final correlation of average gas-side head temperatures for individual coolants. Cylinder A.

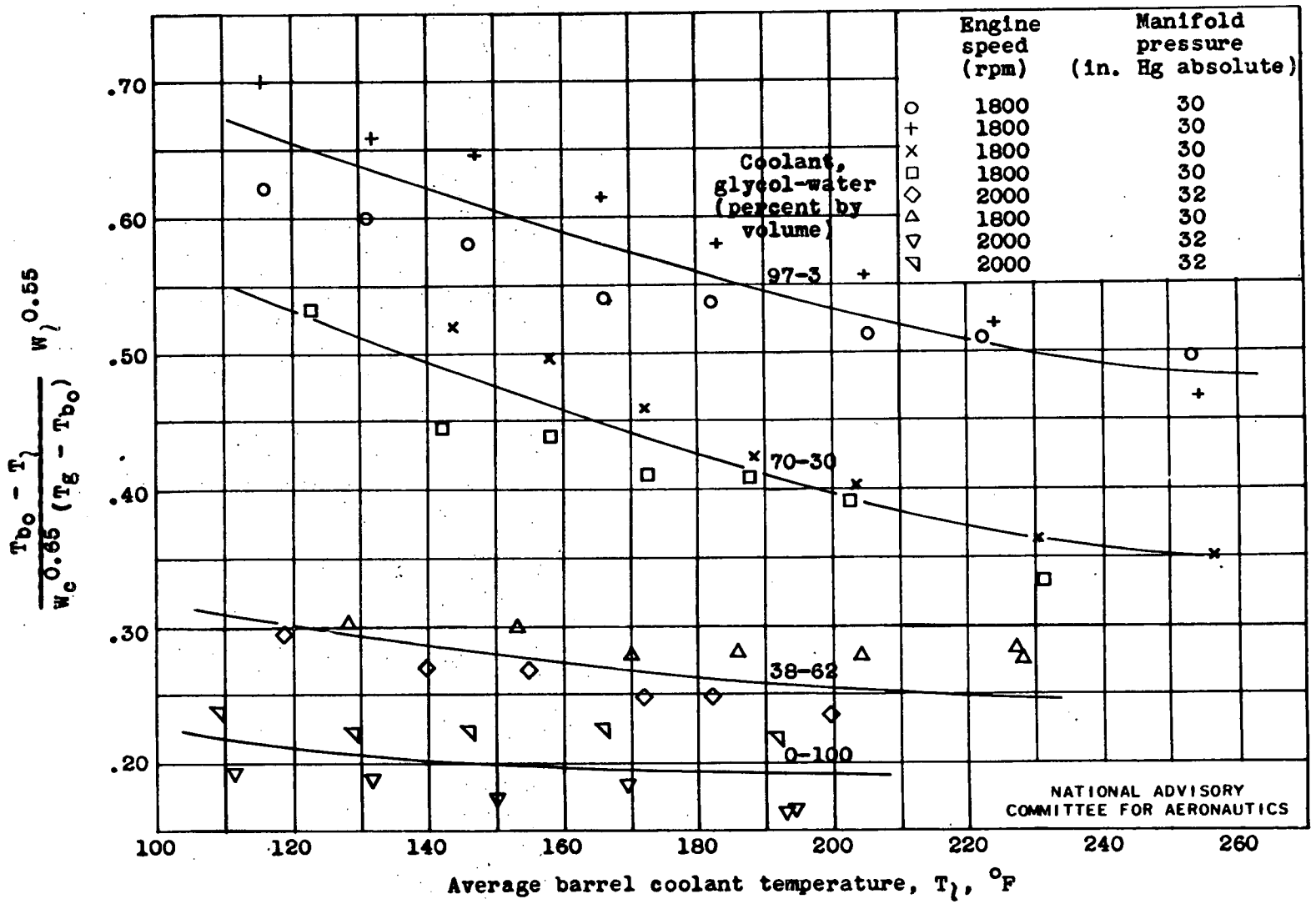

Figure 18.- Final correlation of average liquid-side barrel temperatures for individual coolants. Cylinder A.